AD-A136 468 C-H AND H-H ACTIVATION IN TRANSITION METAL COMPLEXES AND ON SURFACES(U) CORNELL UNIV ITHACA NY DEPT OF CHEMISTRY J Y SAILLARD ET AL. 1983 TR-1 1/2

UNCLASSIFIED N00014-82-K-0576 F/G 7/4 NL

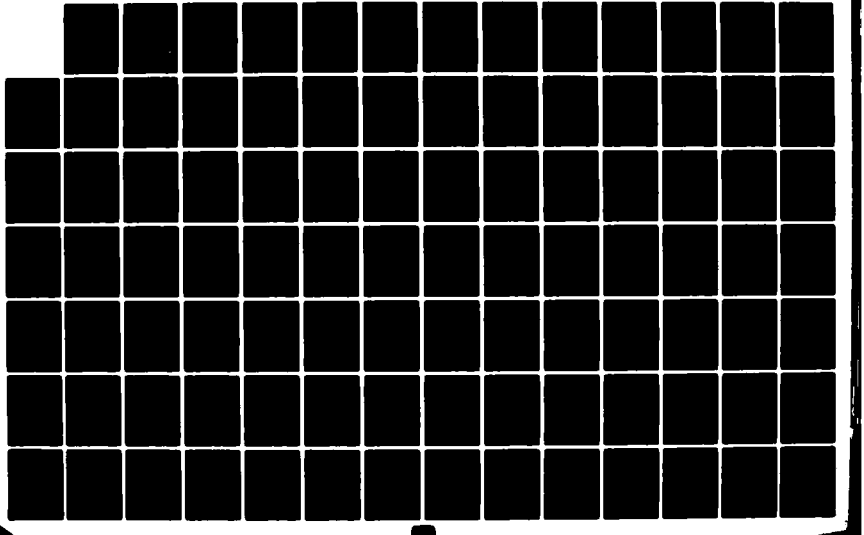

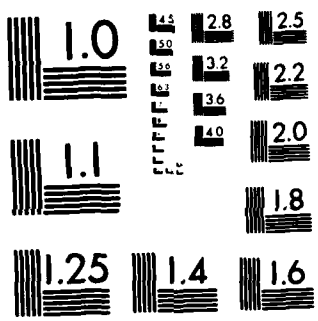

OFFICE OF NAVAL RESEARCH

Research Contract N00014-82-K-0576

TECHNICAL REPORT No. 1

C-H AND H-H ACTIVATION in TRANSITION METAL COMPLEXES AND ON SURFACES

by

Jean-Yves Saillard and Roald Hoffmann

Prepared for Publication

in

the Journal of the American Chemical Society.

Depeartment of Chemistry
Cornell University
Ithaca, N.Y. 14853

C-H AND H-H ACTIVATION IN TRANSITION METAL COMPLEXES AND ON SURFACES

Jean-Yves Saillard and Roald Hoffmann*
Department of Chemistry, Cornell University, Ithaca, New York 14853

The breaking of the H-H bond in H_2 and a C-H bond in CH_4 on both discrete transition metal complexes and on Ni and Ti surfaces is studied, and the essential continuity and similarity of the physical and chemical processes in the two cases is demonstrated. We begin with an orbital analysis of oxidative addition, delineating four basic interactions: H-H or C-H $\sigma \rightarrow M$ electron transfer, the reverse $M \rightarrow \sigma^*$ transfer (both weakening the σ bond, forming the M-H bond), a repulsive interaction between σ and metal filled orbitals, and a rearrangement of electron density at the metal. The molecular cases analyzed in detail are $d^6 ML_5$, $d^8 ML_4$ and $CpM'L$. Coordinative unsaturation is necessary, and consequently $\sigma \rightarrow M$ electron transfer dominates the early stages of the reaction. Steric effects are important for CH_4 reaction. Activation in angular ML_4 or $CpM'L$ is achieved through a destabilized yz

MO, and $d^{10}ML_3$, ML_2 candidates for activation are described. For our study of the surface we develop tools such as projections of the density of states and crystal orbital overlap populations - the extended structure analogues of a population analysis. These allow a clear understanding of what happens when an H_2 or a CH_4 molecule approaches a surface. Because of the higher energy of the occupied metal orbitals on the surface the $M \rightarrow \sigma^*$ interaction leads the reaction. There are great similarities and some differences between the activation acts in a discrete complex and on a surface.

In this paper we will try to understand how an H-H or C-H bond can interact and eventually break in the proximity of one or more transition metal centers. We analyze this problem both for discrete complexes and for a clean metal surface; indeed the most interesting aspect of our study will be the comparison of similarities and differences between the chemistry that goes on in an inorganic complex and on a metal surface.

Let us review the experimental background of this problem. Until recently there was a nice sharp dichotomy in the chemistry of H_2 with transition metal complexes. If H_2 interacted at all, it reacted completely, yielding in an oxidative addition process a metal dihydride, 1. This species was sometimes observed, more often inferred as it was consumed rapidly in some subsequent rapid chemistry.[1] Recently the first well-characterized H_2 com-

1

plex was observed.[2] This is 2, a side-one bonded complex with a d^6 ML_5 fragment. The H-H distance, available from a neutron diffraction study, is 0.75 ± 0.16 Å.

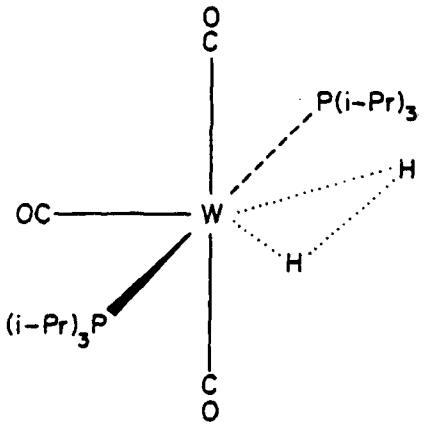

2

For the interaction of a C-H bond with one or more metal atoms the experimental history is much richer. Over the years it has become apparent that a C-H σ bond can interact in a bonding way with a coordinatively unsaturated metal center (16 or less electrons around the metal) and in so doing allow the metal to achieve or approach the stable 18 electron configuration.[3] Unsaturation at the metal and proximity are required. The intermolecular cases, most of which are quite recent, proceed on to oxidative addition, 3.[4]

3

The intramolecular examples, ones in which the interacting alkyl group is somehow tethered to the metal atom, have been revealing in showing us details of the initial states of metal-CH interaction. There is by now an ample store of structural or spectroscopic evidence for intramolecular M-CH interaction with a variety of geometries, coordination numbers and electron counts at one or more metal atoms. Precise structure determinations, utilizing neutron diffraction, show short M to H (and C) contacts, and unusually long C-H bonds (the world's record now stands at 1.19Å[5]). C-H stretching frequencies often are dramatically lowered and C-H coupling constants as well. There is evidence of both linear, 4a and triangular, 4b, interaction geometries.

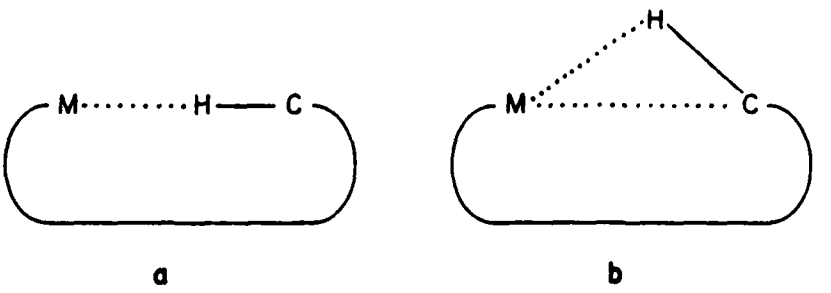

4

H_2 and alkanes are, of course, chemisorbed, dissociated, and reassembled on many transition metal surfaces of varying degrees of cleanliness. In recent times the reactivity of definite crystal planes has been studied in some detail, and we are beginning to gain information on the microscopic structure of the product surface.[6]

Theoretical studies of surfaces and their interaction with molecules are now being done by several groups. We want to single out for special mention here the work of R. Baetzold, E. Shustorovich and E. Muetterties[7] because it anticipates many of the conclusions that we eventually reach about the surface, in particular concerning the role of the substrate σ^* orbitals and the direction of electron flow during surface-substrate interaction. Other theoretical studies will be mentioned in the course of the paper.

Charge Transfer and Bond Making in Oxidative Addition

At the risk of repeating what is obvious let us examine the essential features of oxidative addition, correlating the basic ideas of electron transfer and oxidation, reduction with the way in which these appear in a molecular orbital description of a process.[8]

Drawing 5 is a schematic illustration of the level transformation in a transition metal complex reacting with H_2. The ML_n complex is represented

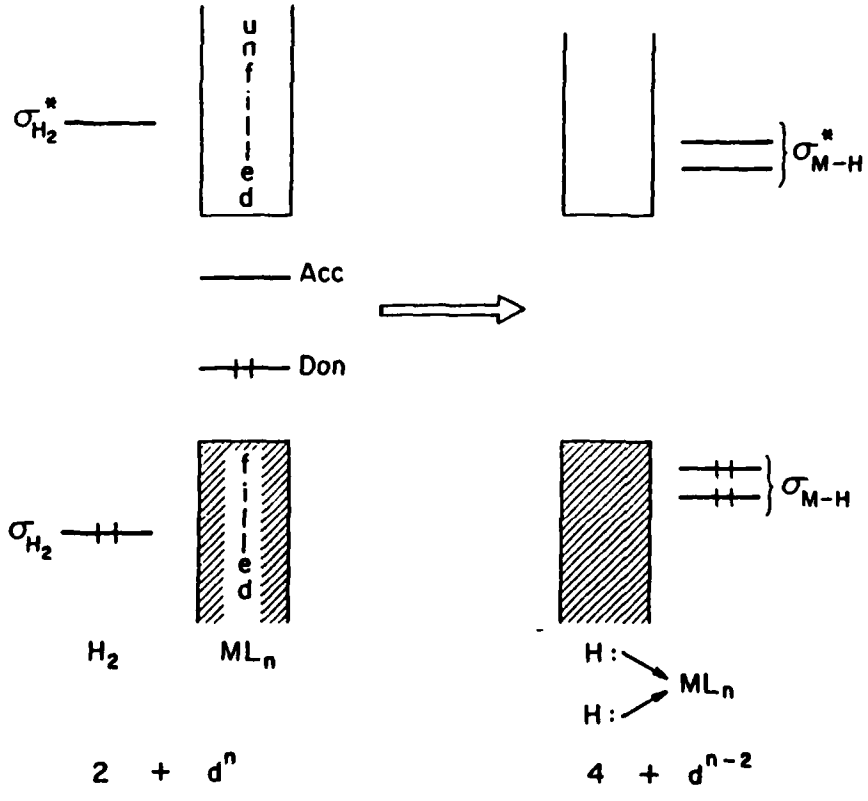

5

by a band of occupied levels and a band of unoccupied ones. The metal surface will be no different. One of the metal filled levels (Don for Donor) and one of the unfilled ones (Acc for Acceptor) is singled out, for reasons which will soon become apparent. At the end of the reaction two new M-H σ bonds form, and of course their corresponding antibonding combinations. In the conventional Wernerian scheme of counting ligands as two-electron σ donors the four electrons of the two new M-H σ bonds are assigned, for electron counting purposes, to the ligands, H^-. It is this convention which makes the metal go from a d^n to a d^{n-2} electron count, and makes us call this reaction an oxidative (at the metal) addition.

Formalisms are convenient fictions which contain a piece of the truth - and it is so sad that people spend a lot of time arguing about the deductions they draw, often ingeniously and artfully, from formalisms, without worrying about their underlying assumptions. The "complex" or dative bonding picture which led to "oxidation at metal" of course is an exaggeration. The M-H σ bonds are in good part covalent. To the extent that they are so, the real d electron population at the metal moves back from d^{n-2} toward d^n. To the extent that it probably never quite gets back to d^n it is still informative to call this an oxidative addition.

What the "oxidative addition" formalism conceals and a molecular orbital picture reveals is that in the course of this reaction there has to be

a two way flow of electron density, from the metal to the new ligands and in the reverse direction.

Consider the M-H σ bonds in the product. In a localized representation they are shown in 6, and the equivalent delocalized picture in 7.

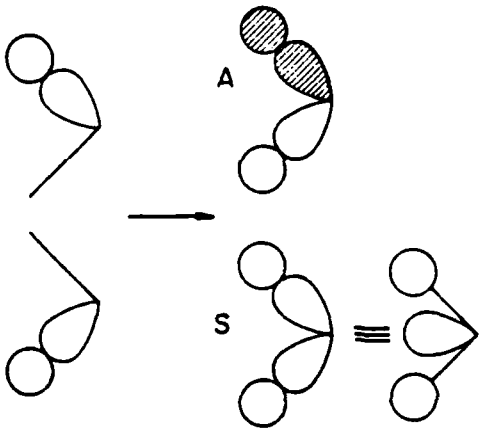

6 7

The delocalized orbitals are labelled as S or A according to their symmetry or antisymmetry with respect to the two-fold axis or mirror that interchanges them.

Where did 7S and 7A originate? They came from the interaction of σ_{H_2} with metal Acc and metal Don with $\sigma^*_{H_2}$. This is shown in 8 and in

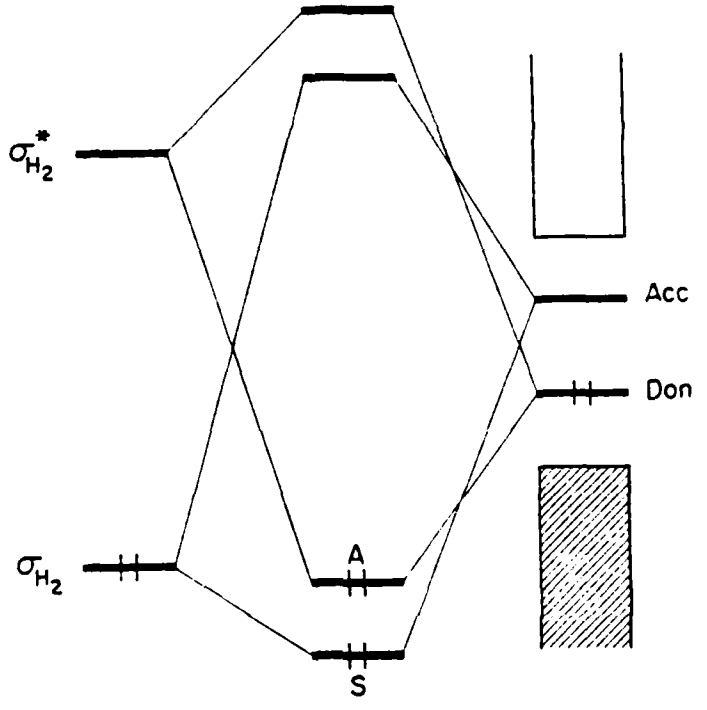

8

another way, focussing on the evolution of the orbitals, in 9. What 9 shows clearly is the two way charge transfer and the coupling of electron transfer and bonding changes. The symmetric M-H combination evolves from σ_{H_2} by mixing in of a metal acceptor orbital of appropriate symmetry. The result is electron transfer <u>from</u> $H_2\sigma$, decreased H-H bonding and increased M-H

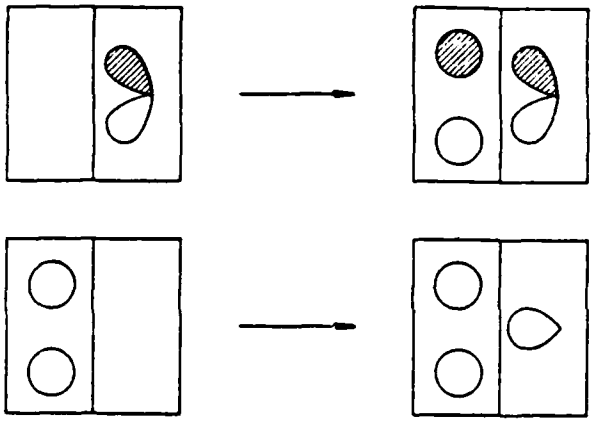

9

bonding. The A combination electron transfer is in the opposite direction, for this orbital is originally on the metal. Electron transfer <u>to</u> $H_2\sigma^*$ has as a consequence decreased H-H bonding and increased M-H bonding.

Note that both these interactions lead to H-H bond weakening and M-H bond formation, even though they accomplish these actions by charge transfer in different directions.

The molecular orbital description makes it clear that when oxidative addition is complete there must have occurred electron transfer from metal to H_2 or RH <u>and</u> in the reverse direction. But there is no requirement that

the electron flow be balanced at every stage of the reaction. In fact the experimental evidence for the requirement of coordinative unsaturation of the metal in activation on discrete complexes makes it clear that in these molecules the important initial electron flow is from H_2 to metal. As we will see metal surfaces may be different.

So far we have identified the two most important bonding interactions between hydrogen molecule or an alkane and a discrete transition metal complex or a metal surface. They are repeated in 10, labeled as (1) and (2) now. These are two-orbital two-electron bonding interactions. Two further interactions must be thought about. Interaction (3) is the two-orbital four-electron perforce destabilizing interaction between filled orbitals of substrate and surface (or complex). It is in this interaction that one-electron theories of the extended Hückel type find what chemists normally call "steric effects". Interaction (3) is destabilizing, and leads to some M-H antibonding. It is the primary source of barriers to C-H activation.

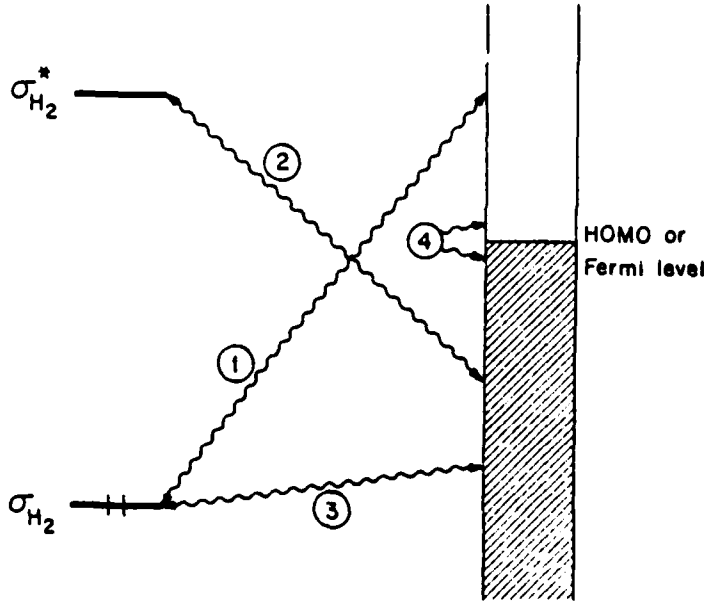

10

In addition to these three interactions, which operate for an ML_n complex as well as for a metal surface, there is another interaction, (4), which is generally important only for metal surfaces, where there are many closely spaced levels. What happens on the surface, as we will see in great detail below, is that some levels, more localized on the surface than in the bulk, and even on the surface distinguished by reaching out toward the substrate, some levels interact to a greater extent than others. They do so, of course, through the primary interactions (1), (2) and (3). But since in a solid or a surface levels are closely spaced around the Fermi level, the net result of such primary interactions of substrate and "surface states" is a shift of electron density between bulk and surface, and even within the surface. This interaction is poorly represented in 10 by (4), but its significance will eventually become clearer as we describe it in more detail later.

We are now ready to proceed with an analysis of several specific cases, to see these interactions in action. But first let us describe the computational methodology we use. This is the extended Hückel method,[9] with particulars described in Appendix 1. There is a special problem which this transparent and simple procedure brings with it. The method is not reliable for bond distance changes, and H_2 in particular is a pathological case in which the two atoms collapse. So the study of potential energy surfaces where H-H or C-H bonds are made or broken would seem to be an inappropriate applica-

tion of the extended Hückel method. In fact this is so, and since we cannot trust the method for bond distances we do not calculate complete potential energy surfaces. Instead we limit ourselves in general to the study of select approaches - for instance an H_2 coming on parallel or perpendicular to a surface - and focus on that aspect of the electronic redistribution which the extended Hückel method from our experience is likely to get right. This is the magnitude and nodal character of orbital interactions.

We also apply consistently the language and formalism of simple perturbation theory, in particular the second order expression for the interaction of two levels:

$$\Delta E = \frac{\left| H_{ij} \right|^2}{E_i^\circ - E_j^\circ}$$

Extended Hückel arguments, especially in the fragment orbital analysis, translate directly into perturbation arguments. It is this combination of extended Hückel calculations, and perturbation theory based thinking within a one-electron frontier orbital picture that makes us feel more sanguine about the results of what would otherwise have been a pretty unreliable calculation.

H_2 and CH_4 as substrates

The orbitals of both molecules are familiar. Within a simple single configuration picture the valence orbitals are filled σ_g in H_2, an $a_1 + t_2$ set in CH_4, and the corresponding unfilled σ_u^* in H_2 and a_1^* and t_2^* in CH_4. The orbital energies as given by the extended Hückel method are shown in Figure 1. The C-H bonding in CH_4 is distributed over the a_1 and t_2 set, but is mainly in the t_2 component. If we focus on that orbital as the C-H bond and then compare CH_4 and H_2 then, as far as energetics are concerned, the two molecules are equally good (poor) acceptors, but CH_4 is a better (but still not good) donor, as its t_2 set is some two eV higher in energy than H_2 σ.

Figure 1 here

The numerator of the perturbation sum, $|H_{ij}|^2$, is not to be forgotten. Coefficients of the relevant orbitals are given in 11. Note first the spectacular difference between the σ_g and σ_u^* H coefficients in H_2. This is a result of including the overlap in the normalization of the molecular orbitals. An immediate consequence is that σ^* orbitals, acting through the numerator of the perturbation expression, will have much more "power" in the interaction. This will compensate sometimes (as we will see, especially

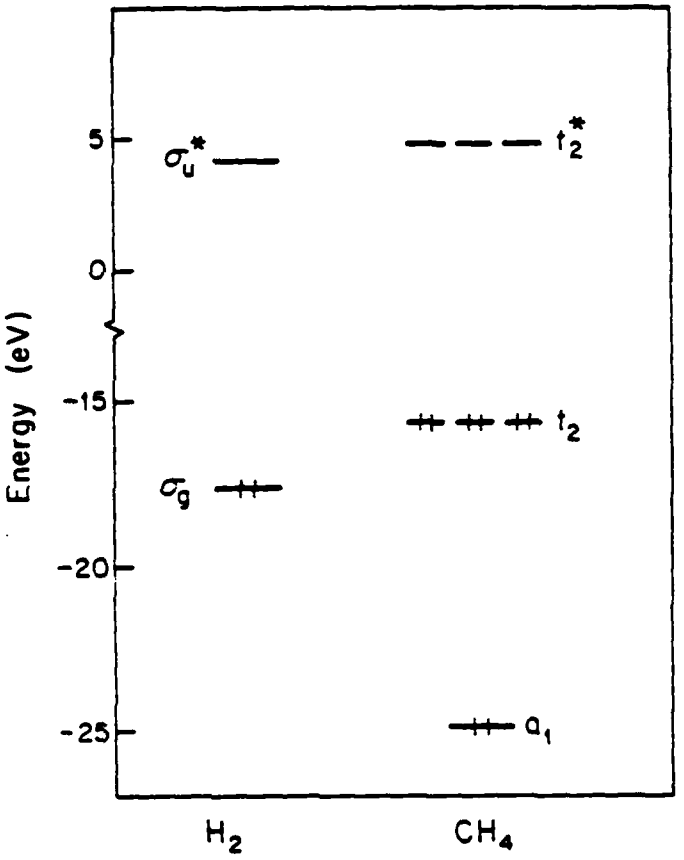

Fig. 1 Frontier orbitals of H_2 and CH_4.

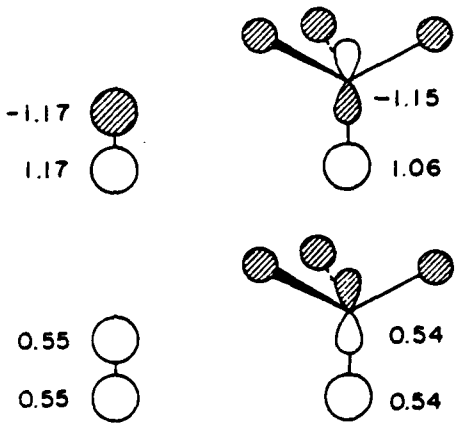

11

on transition metal surfaces) for their very high energy, which, acting through the denominator of the perturbation expression, makes it difficult for them to have much influence. Note the similarity of the effective H coefffcients in CH_4 and H_2.

We are now ready to proceed with calculations on the addition of these molecules to various ML_n fragments. The reader should note that our calculations are not the only ones extant, and that several others have been published.[10]

A Prototype Mononuclear Transition Metal Fragment, $Cr(CO)_5$

Why $Cr(CO)_5$? Complexes of $Cr(CO)_5$ with methane and hexane in in low temperature matrices have been detected.[11] The only well-characterized H_2 complexes $M(CO)_3(PR_3)_2H_2$, M=Mo, W are closely related to $Cr(CO)_5$[2], and many of the cited intramolecular cases of C-H activation can be related back to this model.[5ℓ-t]

The total energy of an H_2 frozen at H-H 0.74 Å approaching a C_{4v} octahedral fragment $Cr(CO)_5$ is shown in Figure 2. Two approach geometries were studied, a "perpendicular" and "parallel" mode. These are sufficiently

Figure 2 here

common in the subsequent discussion that it is best to describe them more precisely in 12 and 13. "Perpendicular" means H-H (or eventually C-H) colinear with the metal atom, "parallel" means turned by 90°, so that both M-H distances are equal. The L_nM-H_2 separation, somewhat arbitrarily, is defined as the distance to near hydrogen in the perpendicular geometry, but to the H-H centroid in the parallel form.

perpendicular

12

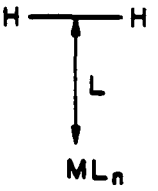

parallel

13

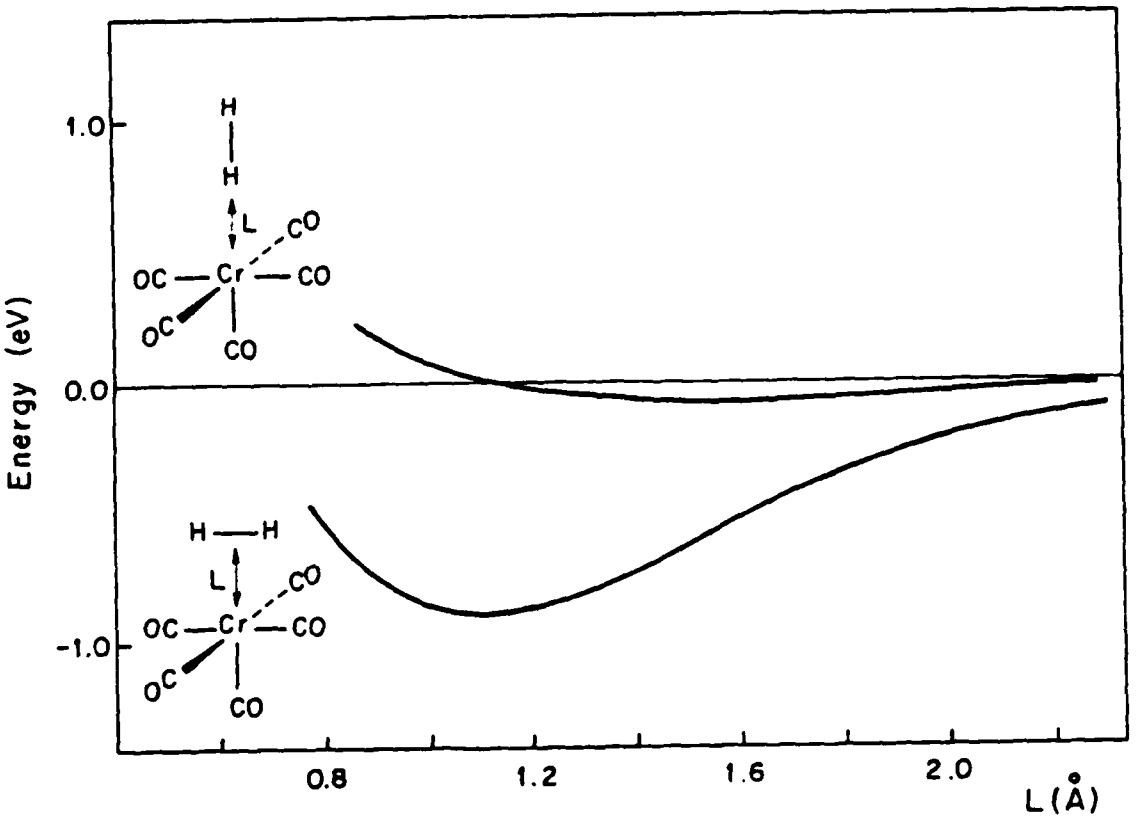

Fig. 2 Total energy along the perpendicular and parallel approaches of H_2 to $Cr(CO)_5$. The common energy zero for both curves is for the two fragments at infinite separation.

The two energy curves are attractive over a substantial range of approach distances, and the parallel minimum is deeper. This is consistent with the single structure known, 2, but why is it so?

A level interaction diagram (Figure 3) is illuminating. Singled out in the middle of the construction are the familiar orbitals of a 16 electron C_{4v}

Figure 3 here

ML_5 fragment - a t_{2g} set below a well-directed a_1 hybrid.[12] In the perpendicular geometry the t_{2g} set is untouched, while both σ_g and σ_u^* interact in a typical three-orbital pattern with ML_5 a_1. The significant bonding mixing is of type (1) in 10, between σ_g and a_1 of $Cr(CO)_5$ in Figure 3. It gives rise to stabilization, but the stabilization is not great as it is underlain by a repulsive base of four-electron destabilizing interactions.

In the parallel geometry the interaction between σ_g and a_1, though somewhat different in spatial configuration, in fact is not significantly worse in overlap. Now a strong interaction of type (2), metal acting as a donor (xz) toward the ligand as acceptor (σ_u^*), is allowed by symmetry, whereas it was forbidden in the perpendicular approach. There is electron transfer from σ (0.110 electrons at L=2.0 Å) and into σ^* (0.032 electrons at L=2.0 Å). No wonder the parallel geometry is preferred.

The situation is changed dramatically if the H-H bond is substituted by C-H of CH_4 (Figures 4 and 5). The perpendicular approach is still attractive, but the parallel one is not, becoming strongly repulsive. The level

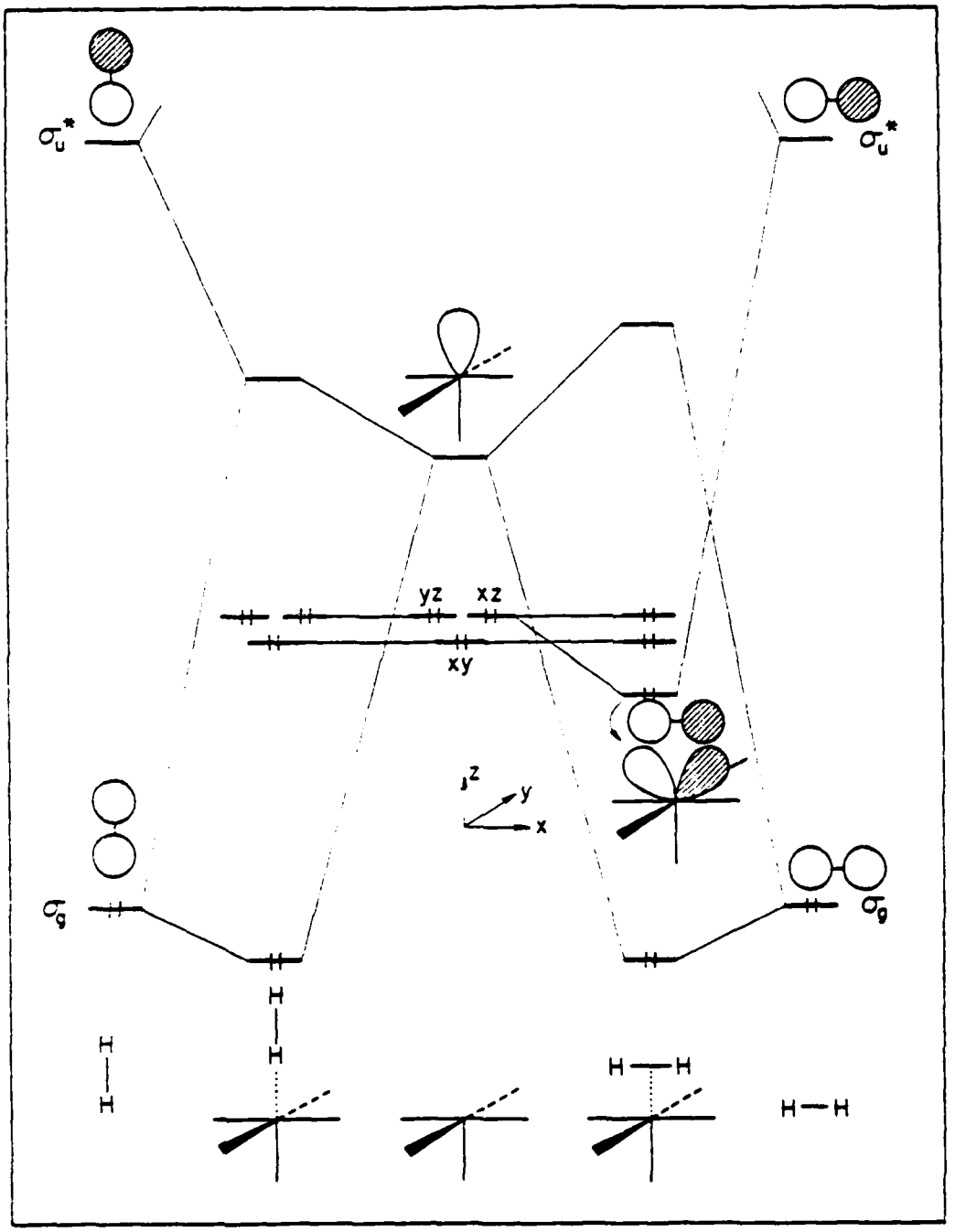

Fig. 3 Interaction diagram for H_2 and $Cr(CO)_5$ for a perpendicular (left) and parallel (right) approach. The diagram is schematic in the position of the σ_g and σ_u^* levels before and after interaction.

analysis reveals that the origin of stabilization in the perpendicular approach

Figures 4 and 5 here

is the same for CH_4 as H_2. In the parallel geometry something different is happening, for instead of xz going down in energy (H_2), in the case of methane both xz and yz go up. The reason for this behavior may be seen from the fragment overlaps (at L=2.0 Å) in 14.

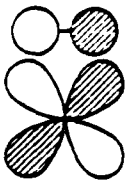

$\langle xz \mid \sigma_u^* \rangle = 0.15$

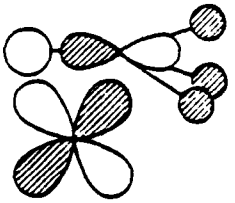

$\langle xz \mid \sigma^* \rangle = 0.04$

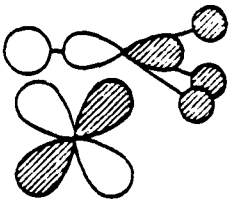

14

$\langle xz \mid \sigma \rangle = 0.08$

The H_2 xz - σ* overlap is big, but that of the corresponding σ* component of CH_4 is small. The metal d orbital is mismatched with the methane, and samples the rear of the CH σ* combination. Furthermore, there is a substantial overlap between metal xz and the occupied C-H σ orbital. In fact this repulsive effect dominates pushing xz up in energy (Figure 5) as it interacts

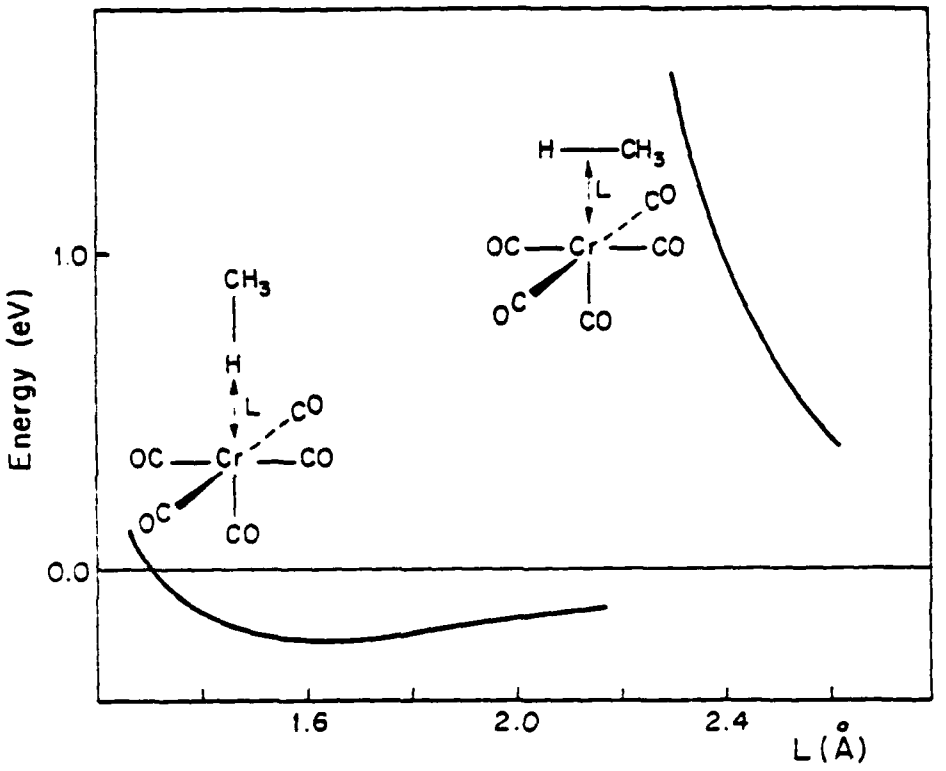

Fig. 4 Total energy for perpendicular and parallel approaches of CH_4 to Cr $(CO)_5$. The common energy zero for both curves is for both fragments at infinite separation.

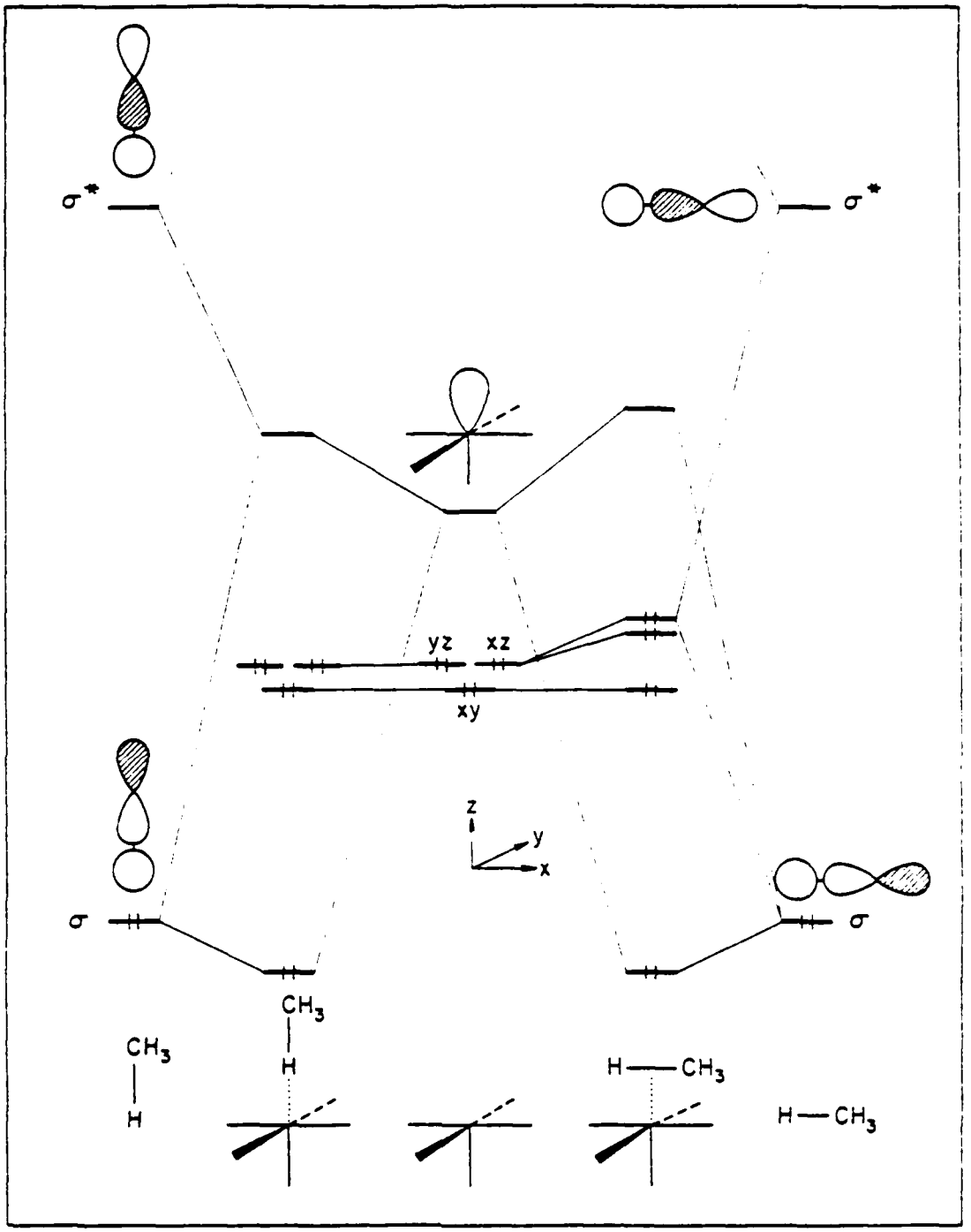

Fig. 5 Interaction diagram, schematic at the top and bottom of the energy range, for perpendicular (left) and parallel (right) approaches of CH_4 to $Cr(CO)_5$.

more with C-H σ than with σ^*. The metal yz orbital also goes up as a result of a similar four electron destabilization with another member of the t_2 set.

What we have is the dominance of two orbital four electron repulsions over the attractive bonding forces. We think that we can identify the repulsive effects, as safely as one can do it within the framework of a one electron theory, with steric effects.

Thus, when a methane approaches a $Cr(CO)_5$ in a parallel geometry the steric problems of that approach overrule the favorable geometric arrangement. Rotation of the methyl group around the H-C bond does not alleviate the trouble. Can a geometry intermediate between parallel and perpendicular achieve a compromise?

We tried 15 and 16, in various geometries. Stabilization was achieved

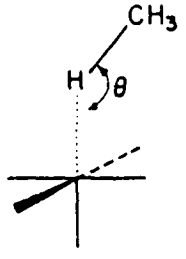

15

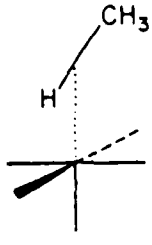

16

for some geometries, for instance at M-H 2.0 Å, 15 is bound for all $\theta \leq 130^{\circ}$. But the perpendicular configuration, $\theta = 180^{\circ}$, is most stable. These are intermolecular cases, and we are certain that in special intramolecular geometries, where the C-H bond is so suspended near the metal that steric effects are minimized, that an appropriate triangular geometry with partial M-H and M-C bonding is attainable.

A particularly interesting example of intramolecular interaction occurs in the series of 16 electron, near octahedral complexes of type 17. These

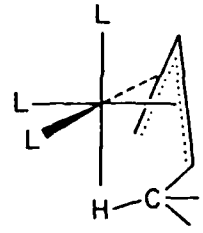

17

exhibit short M···H and M···C contacts associated with fluxional behavior of the H atom[5a,t-v]. Previous extended Hückel calculations on the model $[Co(\eta^3\text{ - alkenyl})(PH_3)_3]^{2+}$ have pointed out a low lying orbital in which both M···H and M···C interactions are bonding[5q]. Our calculation on the isoelectronic $[Fe(\eta^3\text{ - alkenyl})(CO)_3]^{+}$ complex shows similar results: two relatively delocalized σ_{CH} orbitals of the methyl group are stabilized by the metal LUMO. In the two corresponding bonding MO's, the overlap populations are 0.060 for M-H and 0.030 for M-C. The corresponding values

for the total overlap populations are 0.075 and 0.006 respectively. Despite the short M-C distance, there is weak interaction. The reason is that the bonding attraction between the accepting hybrid orbital and the σ_{CH} bond is balanced by a secondary H-C antibonding effect, a consequence of the bonding interaction between the metal orbital and the polyenyl π system.

d^8 ML_4 and CpML Systems for Activing C-H Bonds

Short M-H contacts have been shown to exist in planar or near planar 16 electron complexes of type 18.[5d-k]

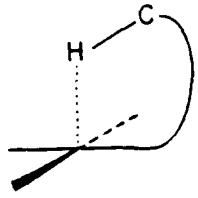

18

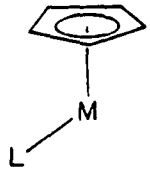

19

Although the accuracy of the H atom positions is poor, the X-ray crystallographic results suggest that the M-H distances lie in the range 2.3-3.0 Å,[5d-f,j] substantially longer and weaker than the corresponding distances in ML_6 complexes. More interesting, perhaps, is the fact that we can place in the d^8ML_4 category the recent exciting cases of C-H activation using the CpML fragment, M=Rh, Ir, 19.[4a-c]

Our model study examined the approach of H_2 and CH_4 to square planar and angular $Rh(CO)_4^+$ fragments, 20 and 21.

20

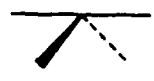

21

Figure 6 shows the computed total energy curves for H_2. Both approaches to the square planar fragment are repulsive. At large separations the perpendicular approach is preferred, in agreement with previous calculations by Sevin[10a] and by

Figure 6 here

Dedieu and Strich[10b]. When the square planar fragment 20 is bent back to the angular one 21, the parallel approach is greatly stabilized.

The reasons for this behavior are made clear by examining the frontier orbitals of 20 and 21,[13] and comparing them to those of the ML_5 fragment, $Cr(CO)_5$. This is done in 22. The crucial difference between d^8 square planar ML_4 and d^6 ML_5 is the presence of the occupied z^2 in the former,

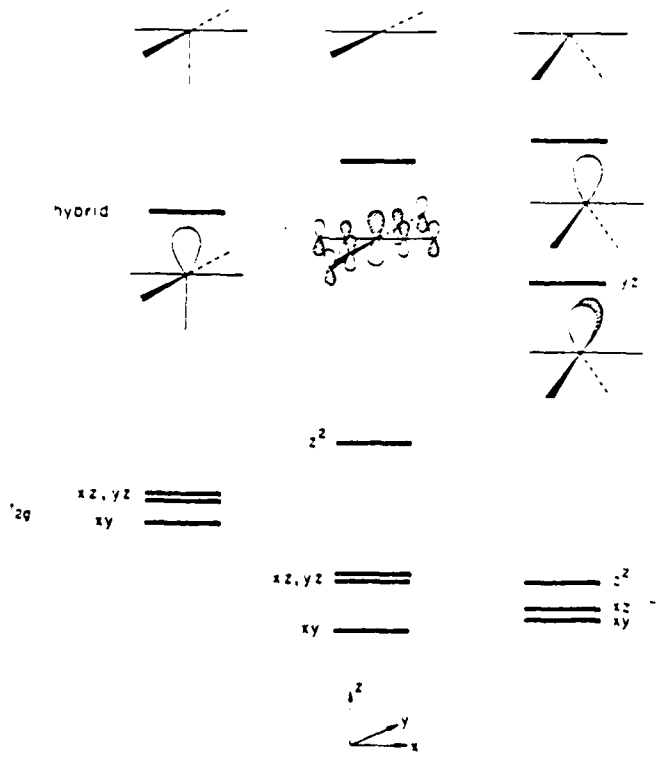

22

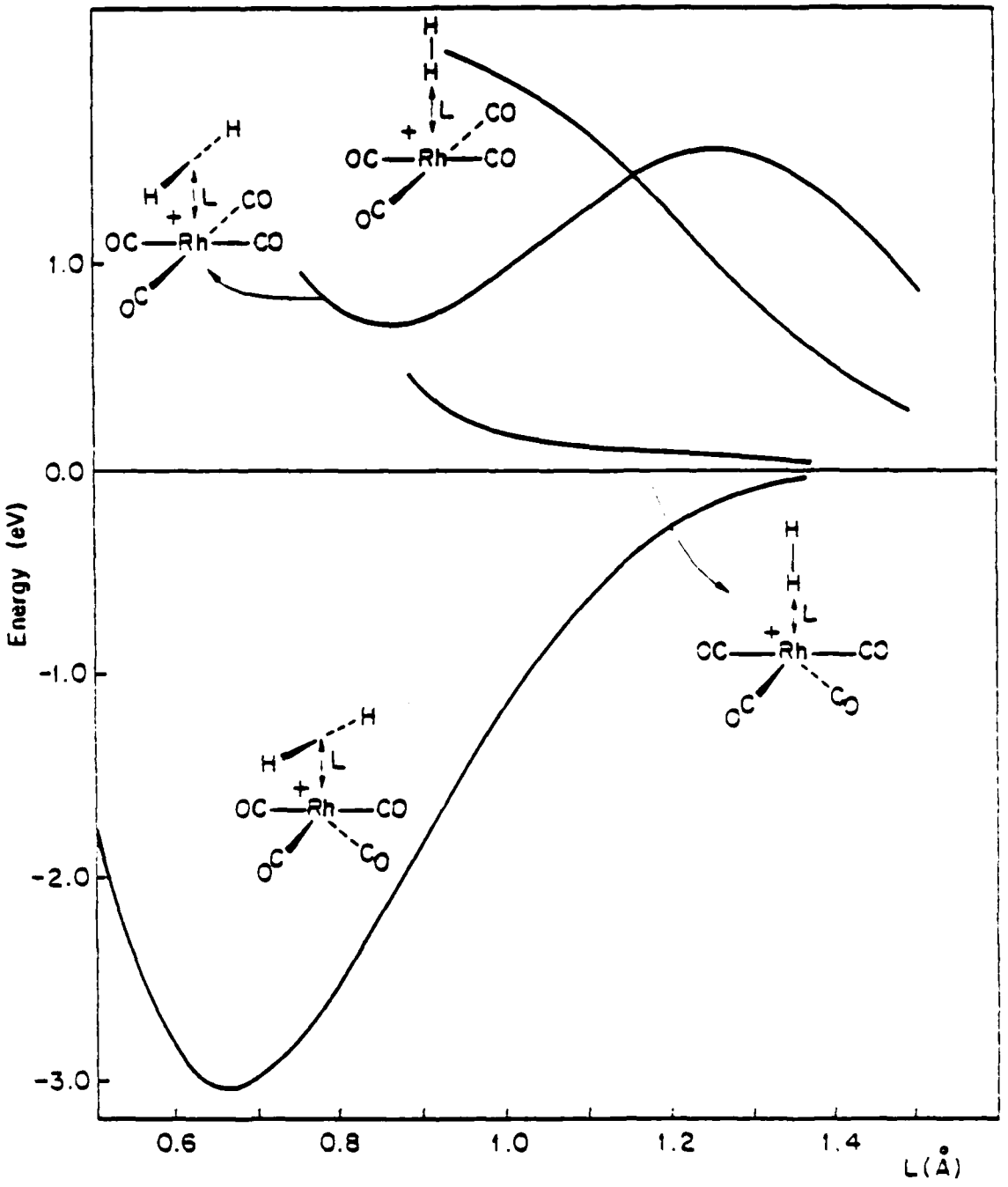

Fig. 6 Total energy for perpendicular and parallel approaches of H_2 to a square planar and angular Rh $(CO)_4^+$. The common energy zero for all curves is at infinite separation of the fragments.

and the very different makeup of the LUMO. The z^2 orbital introduces an additional high-lying orbital of axial symmetry, capable of interaction with σ and σ^* of H_2 in the perpendicular geometry, with σ in the parallel one. The dominant effect is the four-electron destabilizing one, and this is what makes the two square-planar approaches in Figure 6 unfavorable. The acceptor orbital of ML_4 is a poor counterpart of the ML_5 hybrid. The ML_4 orbital which is the LUMO is only 15% metal p, and predominantly ligand π^*. Not suprisingly, given what we know about the chemistry of square-planar d^8 complexes, the coordinative unsaturation or acceptor power of square-planar ML_4 is not strongly developed.

Much changes when two <u>trans</u> ligands in square-planar ML_4 are bent back to give the angular fragment <u>21</u>. The LUMO becomes a hybrid more localized on the metal, and resembling more the LUMO of ML_5. And most importantly the yz orbital, the one which lies in both the plane of deformation and the plane of H_2 approach, is destabilized (thus moving it closer in energy to σ_u^* of H_2, with which it interacts) and hybridized away from the fragment (thus providing better overlap with σ_u^* of H_2). It is no wonder the stabilization shown in Figure 6 is so great - one has moved part-way toward the product geometry of oxidative addition. The deformation toward an angular fragment has activated ML_4 for the reaction, a point noted and discussed in detail by Sevin and by Dedieu and Strich.[10] We will soon see the relationship of

this phenomenon to the observation of CH activation by CpML intermediates.

We have also calculated potential energy curves for the approach of methane to $Rh(CO)_4^+$. The perpendicular approaches resemble those of H_2. The parallel ones are dominated by steric repulsion, so much so that even the very attractive approach of H_2 to angular ML_4 is transformed into a repulsive one in the case of methane.

The observation of short M-H contacts in complexes of type 18 seems in disagreement with our repulsive curves of Figure 6. One could argue that this is the consequence of the choice of carbonyl ligands in our model calculations. Complexes of the type 18 always carry donor ligands such as phosphines or halides. So we did the same calculations replacing the four carbonyls by chlorides. This substitution in planar ML_4 fragments is well known. The main result is a moderate destabilization of the t_{2g} set (xy, xz, yz) and a large destabilization of z, which, however, becomes 85% localized on the metal. The z^2 orbital remains unchanged. As the interaction between ML_4 and H_2 or CH_4 is dominated by the $z^2\sigma_{H_2}$ repulsion, the four E=f(L) curves remain still repulsive, even if they are less so.

A careful examination of the structures of type 18 show that their M-C chains, because of their steric encumbrance and their partial rigidity are forced to lie in a plane roughly perpendicular to the ML_4 plane, bringing a C-H bond in proximity to the metal. The compounds will minimize M···C-H re-

pulsion by bringing the H atom into an axial position (leading to a positive M...H overlap population) and the C atom as far away as possible (thus minimizing the M•••C negative overlap population). Our calculations on the model 23

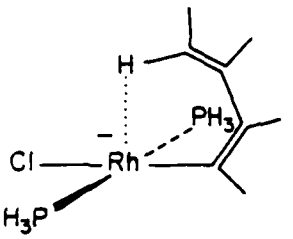

23

give overlap population values of +0.025 for Rh-H and -0.094 for the Rh-C, the corresponding interatomic distance being respectively 1.78 and 2.75 Å. The total M-H-C overlap population is negative, in agreement with a corresponding destabilizing interaction. Our conclusion is in agreement with the structural work of Echols and Dennis[5g] who suggested that in the planar pyrozolyl Ni complexes, there is no M•••H short contact if the molecule is sterically free to avoid it.

Our next goal is to understand the activation of methane by CpML intermediates, such as are thought to be created in the studies of Bergman, Graham, Jones and their coworkers. From a theoretical point of view the

isolobal analogy $d^8ML_4 \leftrightarrow d^8CpM'L$, 24 ↔ 25 is obvious,[14] but does it in fact hold up?

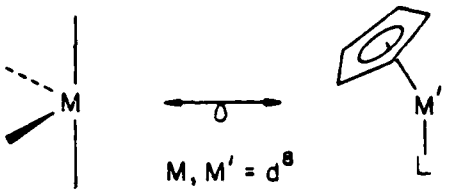

24 **25**

To answer this question we constructed a hypothetical reaction coordinate for the oxidative addition of CH_4 to $Rh(CO)_4^+$ and CpRhCO, 26. We are

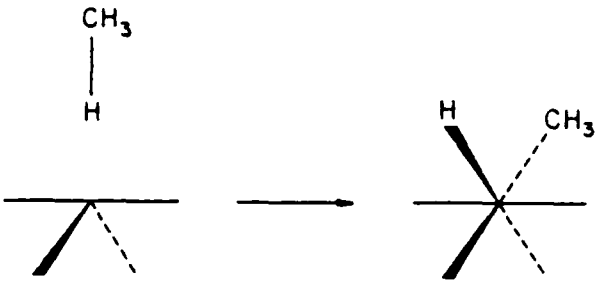

26

not able, as we said above, to calculate a realistic path with the extended Hückel method. Better calculations will have to do that. What we did was to make a linear transit between a point on the perpendicular approach (Rh-H 1.755 Å, corresponding to the minimum on the E(L) curve) and an idealized octahedral product geometry (Rh-H 1.6 Å, Rh-C 1.95 Å). The transit is certainly not optimal, but does contain the essential features of

any reasonable reaction coordinate, for instance reorientation of the methyl group to point toward the metal.

A glance at Figure 7, the comparison of the CpRh $CO(CH_4)$ and $Rh(CO)_4^+(CH_4)$ transits, shows how well the isolobal analogy works. Great similarity is also seen in the Walsh diagram for the two cases. Given the

Figure 7 here

validity of the analogy we would like to go back to the somewhat more symmetrical $Rh(CO)_4^+$ model to see how activation comes about.

A diagram showing the evolution of the critical energy levels along the reaction coordinate, i.e. a simplified Walsh diagram for angular $Rh(CO)_4^+$ and CH_4, is shown in Figure 8. The interacting fragment levels are not much

Figure 8 here

perturbed in the beginning of the reaction (left side of Figure 8). Compare with 22: at low energy in $ML_4 + CH_4$ are xz, xy and z^2, higher is the occupied yz. The final product is a typical octahedral complex with an occupied t_{2g} set. One of the bunch of four highest occupied orbitals is mostly metal - H, CH_3 bonding.

When we use a square-planar ML_4 fragment the calculated barrier to oxidative addition is substantially higher. We can trace the difference, i.e.

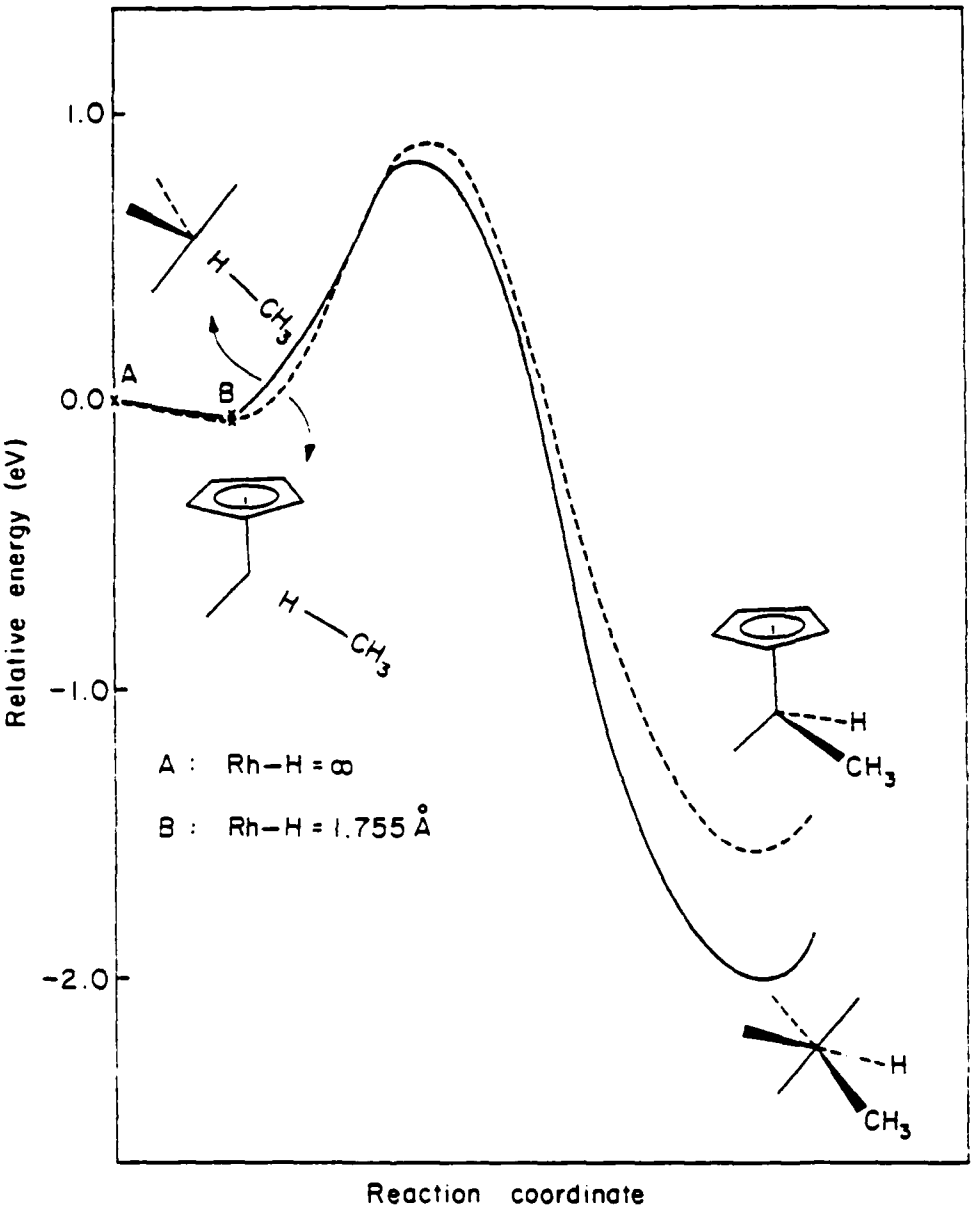

Fig. 7 A comparison of computed potential energy curves for hypothetical oxidative addition reaction coordinates of CH_4 to CpRh (CO) and Rh $(CO)_4^+$. Both molecules are referred to the same energy zero when at infinite separation.

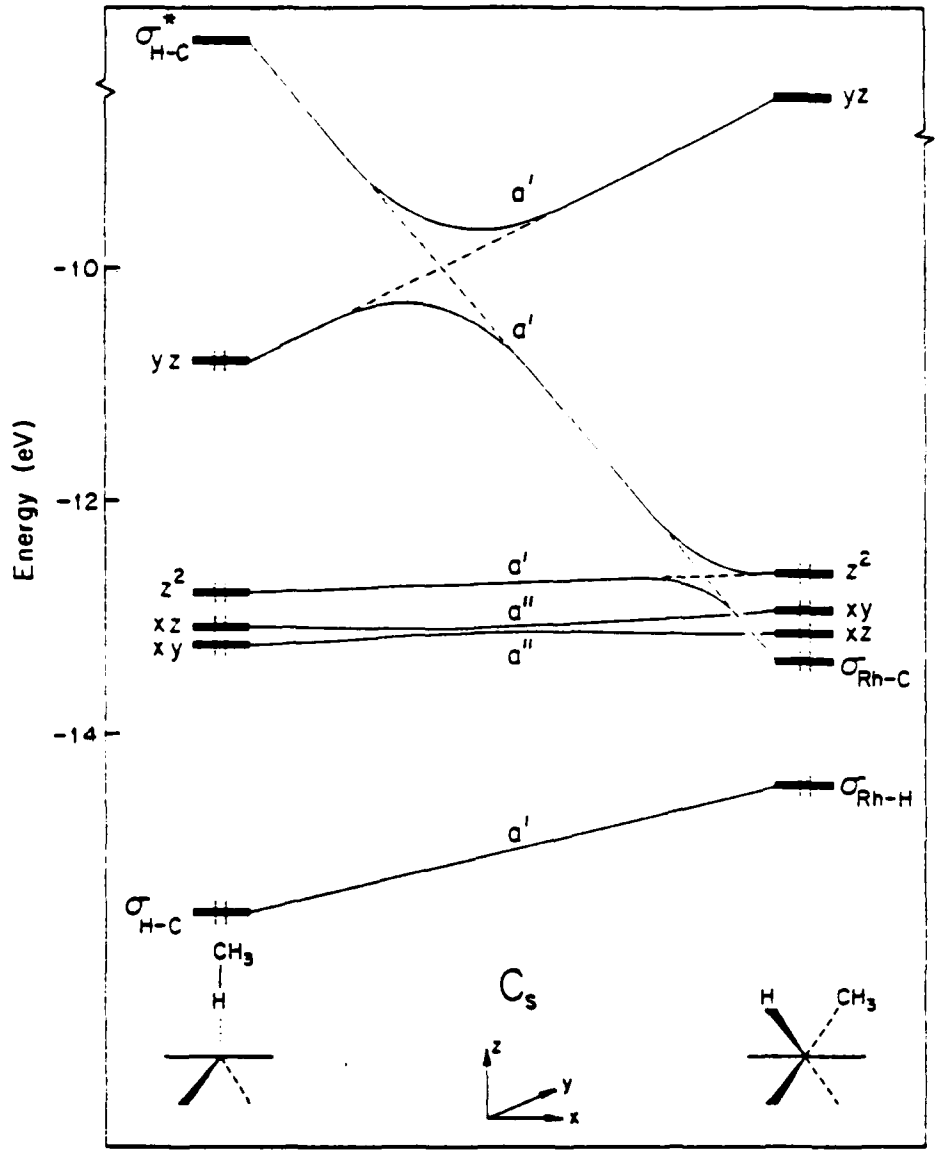

Fig. 8 The evolution of the important energy levels along the oxidative addition reaction coordinate for Rh $(CO)_4^+$ and CH_4.

the lowering of the activation energy when addition takes place to the angular fragment (or to CpML) to the higher energy of the yz orbital in the latter.

It is worthwhile at this point to draw the necessary connection between oxidative addition and its microscopic reverse, reductive elimination. The latter reaction has been studied theoretically in some detail by us and by others.[15] The essence of what happens in reductive elimination is that one of the two M-R σ bond combinations goes down to the new R-R σ bond, 27, while the other combination wants to correlate to R-R σ^*,

27

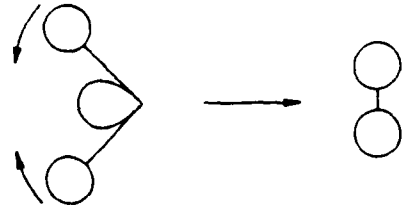

28

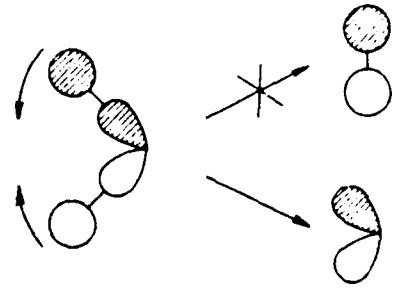

but cannot, 28. Instead it correlates to a metal orbital. We are describing in words the avoided crossing so clearly visible at the top of Figure 8 and

reproduced schematically in 29 below.

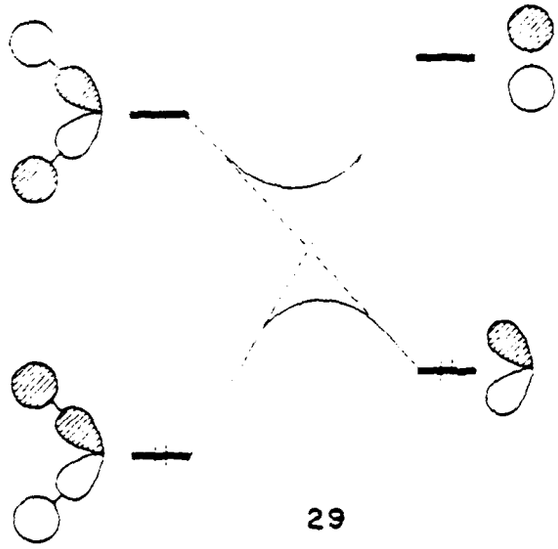

29

It now becomes clear that the higher the metal yz, the higher the heat of the reductive elimination (left to right in 29), but also the lower the activation energy for oxidative addition (right to left in 29). The difference between the square-planar and angular ML_4 fragments lies in the energy of the yz orbital. CpML is perforce related to the angular, and not to the square-planar ML_4 fragment, since a cyclopentadienyl must electronically and sterically be the equivalent of three facial and not meridional ligands.

For the ML_4 case we calculate an activation energy for oxidative addition of 0.92 eV. This value can be reduced farther if a different starting point for the transit is chosen.

Given the importance of a high-lying yz orbital we can try to think of other coordination geometries that enforce such a circumstance. The $d^{10}ML_3$ system comes to mind. If it is forced to be pyramidal, as in 30a or b, then it possesses a high-lying occupied xz, yz pair,[12,16] propitious for a low ac-

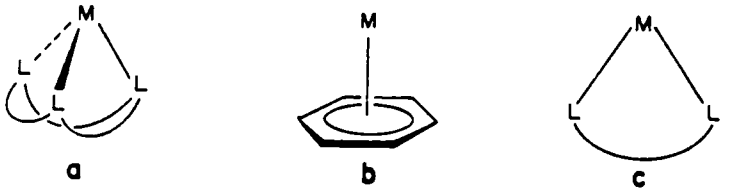

30

tivation energy for oxidative addition. Our calculations on a Rh(benzene)$^-$ + CH_4 model give a barrier of 0.74 eV, starting the transit from an M-H of 1.6 Å. Another system with a high-lying yz level is $d^{10}ML_2$, 30c. A calculation on $Rh(CO)_2^-$ addition also gives a low activation energy. We think that such complexes merit investigation as possible C-H activating systems.

Metals and Metal Surfaces

In principle we could build up toward a metal surface slowly, by examining a progression of clusters of increasing nuclearity, 31.

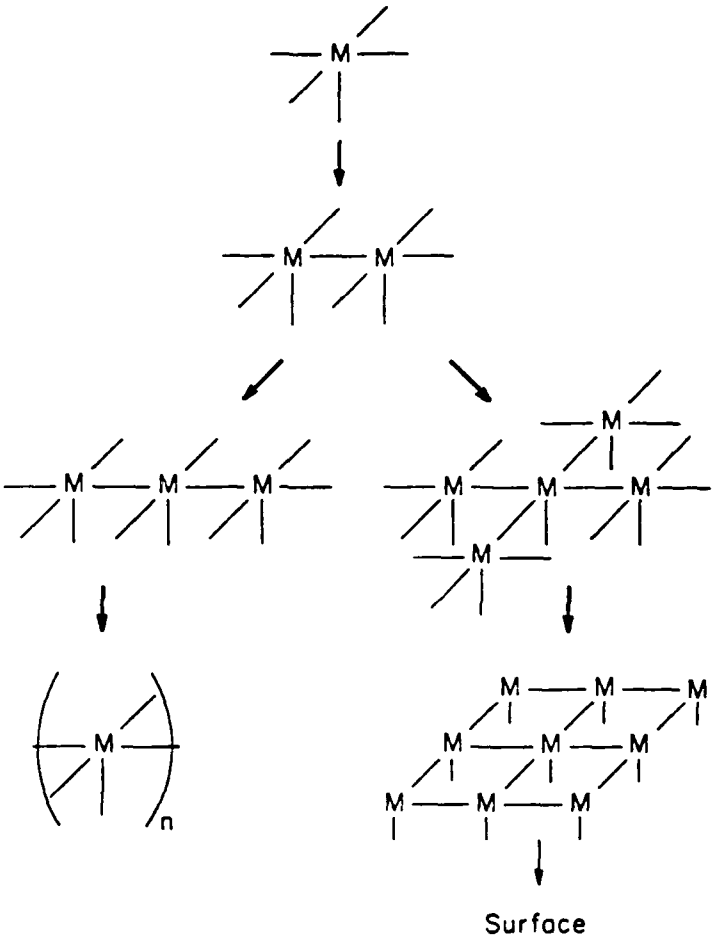

31

As one does this the levels multiply quickly. We strain to find frontier orbital arguments in which all or most of the responsibility for some basic act of chemical reactivity is placed on one or a subset of frontier molecular orbitals.

The perturbation theory based language obviously remains valid, it just seems that one is doing more work than necessary to trace down the important interactions. There must be a way of thinking about chemical reactivity and structure for infinite extended one-, two-, and three-dimensional materials which deals from the beginning in the properties of bunches of levels and not discrete levels.

Such ways of thinking exist, of necessity cast in the language of solid state physics.[17] That language is not too difficult to learn, for in fact most of the concepts, though bearing different names, have a one-to-one correspondence with constructs familiar in theoretical chemistry. So instead of levels of different point group symmetry, one has bands of levels distinguished by a translational symmetry label which happens to be a vector in reciprocal space, in $\underline{k}$ space. The Fermi level is the HOMO, etc. The key to thinking about groups of levels is the density of states, DOS(E), the relative number of states in a given energy interval.

A typical density of states curve for bulk Ni, calculated by the same extended Hückel method as we use for complexes is shown in Figure 9. Note the "d band", largely metal 3d, between -8 and -12 eV. Above it is a broad s and p band, the bottom of which penetrates substantially into the d band. In fact at the Fermi level the populations of the various levels are

Figure 9 here

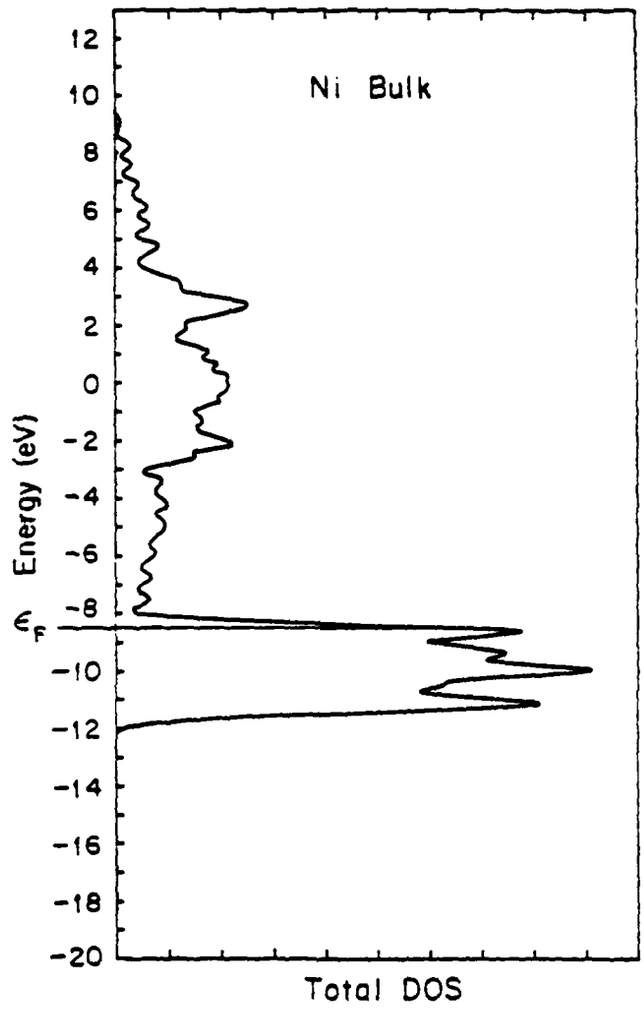

Fig. 9 Density of states of bulk Ni.

as follows: $d^{9.15}s^{0.62}p^{0.23}$. Thus the s band is one third filled.[18]

The bulk Ni density of states is characteristic of the rest of the transition series. In Figure 10 we show the d band width and the Fermi level across the first transition series. The Fermi level falls slowly across

Figure 10 here

the transition series. Its calculated value exceeds the observed work function of the metal by ~3 eV, which is a typical error of the extended Hückel procedure.

In our discussion of the bonding of molecules to surfaces we have found useful a measure of bonding common in theoretical chemistry, but not often utilized in solid state physics. This is the Mulliken overlap population between two atoms. In thinking about extended structures it is necessary to think about groups of levels, so the relevant quantity is the overlap population weighted density of states, i.e. the relative number of levels in a given energy interval weighted by the contribution these levels make to the overlap population for a specified bond.[21] We have called these curves COOP curves (for Crystal Orbital Overlap Population). Their integral up to a specified Fermi level is the total overlap population for the given electron count.

In preparation for our use of COOP curves let's show one, for Ni-Ni bonding in bulk Ni, Figure 11. The bottom of the d band is metal-metal

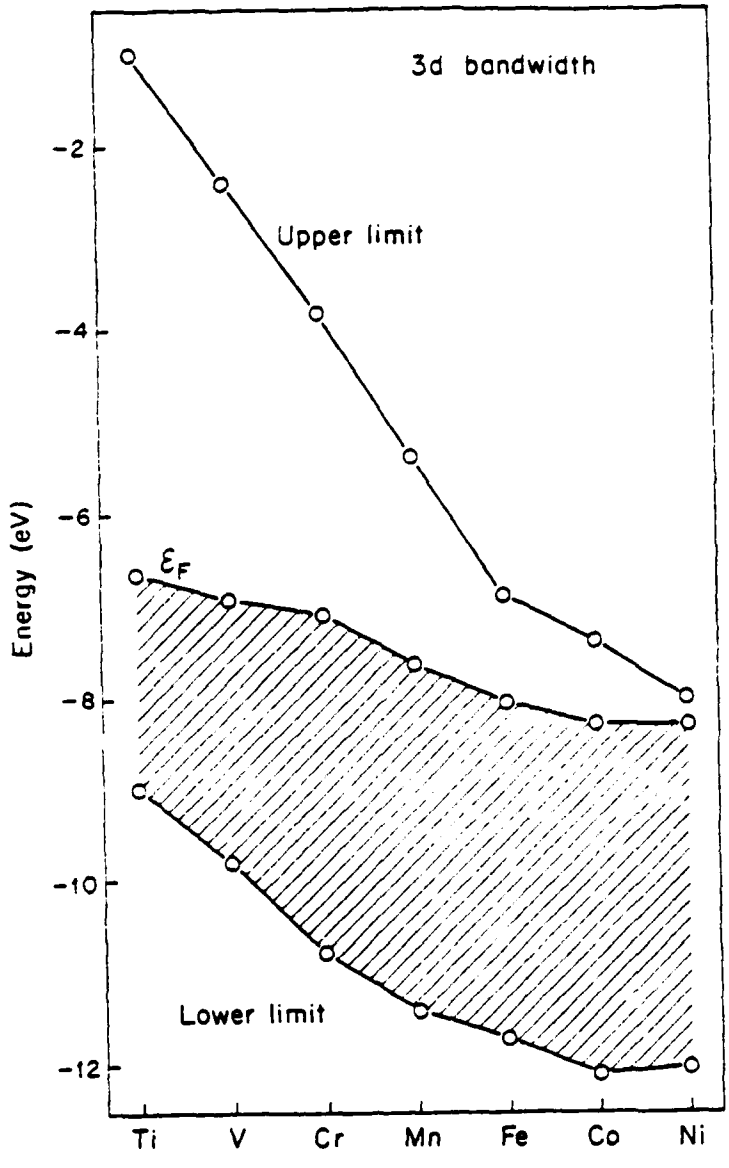

Fig. 10 3d band width and position of the Fermi level, as computed by the extended Hückel method, for the first transition series.

Figure 11 here

bonding, the top metal-metal antibonding. Similarly for the s, p band. This is all as expected. The total Ni-Ni overlap population is 0.107 at the Fermi level.

We now move to the Ni surface. The one we have chosen is (111), a closely packed surface. To take full advantage of translational periodicity we must in fact take a film or slab of finite thickness, a typical tactic in solid state theoretical approaches to surfaces. The thickness of the film should be such as to ensure that it approximates a real surface, yet also the thickness must be kept small for reasons of computational economy. Appendix 2 details our studies of films varying in thickness from a monolayer to 5 layers, and how we settled on 3 or 4 layers as a reasonable approximation to a surface. We have used a four layer film in our studies of H_2 chemisorption, and a three layer film for CH_4 activation. The four layer film is shown schematically in 32.

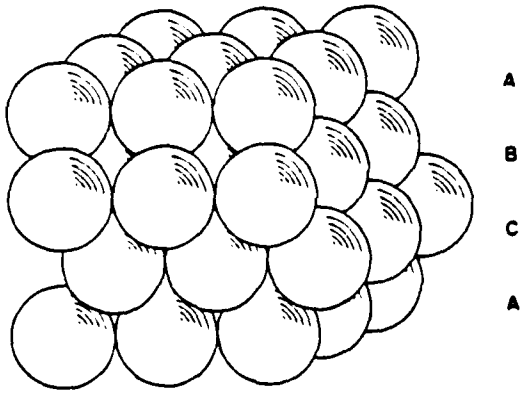

32

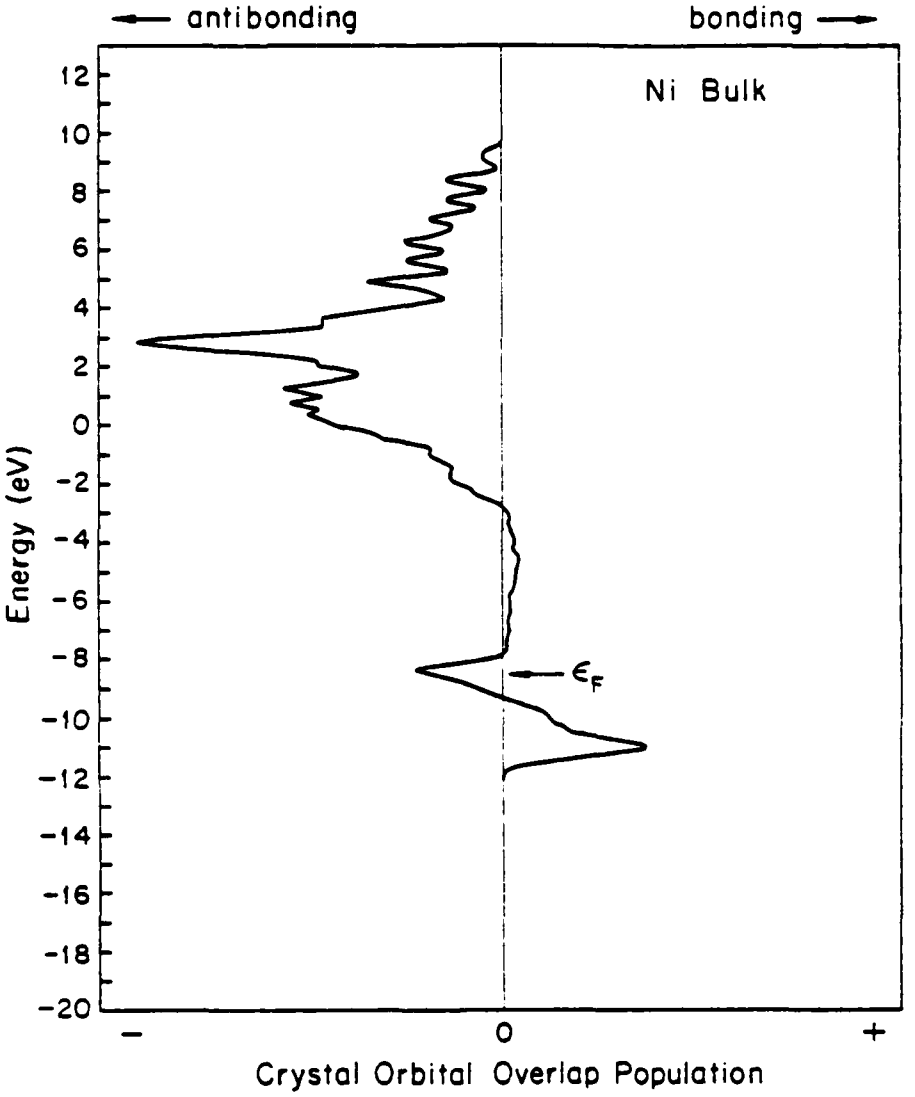

Fig. 11 Crystal Orbital Overlap Population (COOP) curve for bulk Ni.

The four-layer film has two identical surface-like layers and two identical inner or bulk-like layer. Figure 12 shows the total density of states and its projection or partition among the surface and inner layers. Note that

Figure 12 here

the states in the surface layer have somewhat less dispersion, i.e. form narrower bands. This is true for both the d and the s, p band. The reason for this is simply that the surface atoms have less nearest neighbors (9) compared to the inner atoms (12). The number of nearest neighbors affects the number of interactions or overlap available to an atom, and it is the overlap which eventually controls the band width.

This trivial argument, summarized very schematically in 33, has a nontrivial consequence. If we plot for a given band structure, say that of Ni, the relative number of electrons as one proceeds to fill the band, it is clear that the "bulk" like layer will fill first. The bulk will be negative relative to the surface. Then at about half-filling the two layers, bulk and surface will be equally filled. As we fill past this point the surface will become negative. The schematic plot of relative electron distribution as a function of electron count is shown in 34, and is supported by our computations.

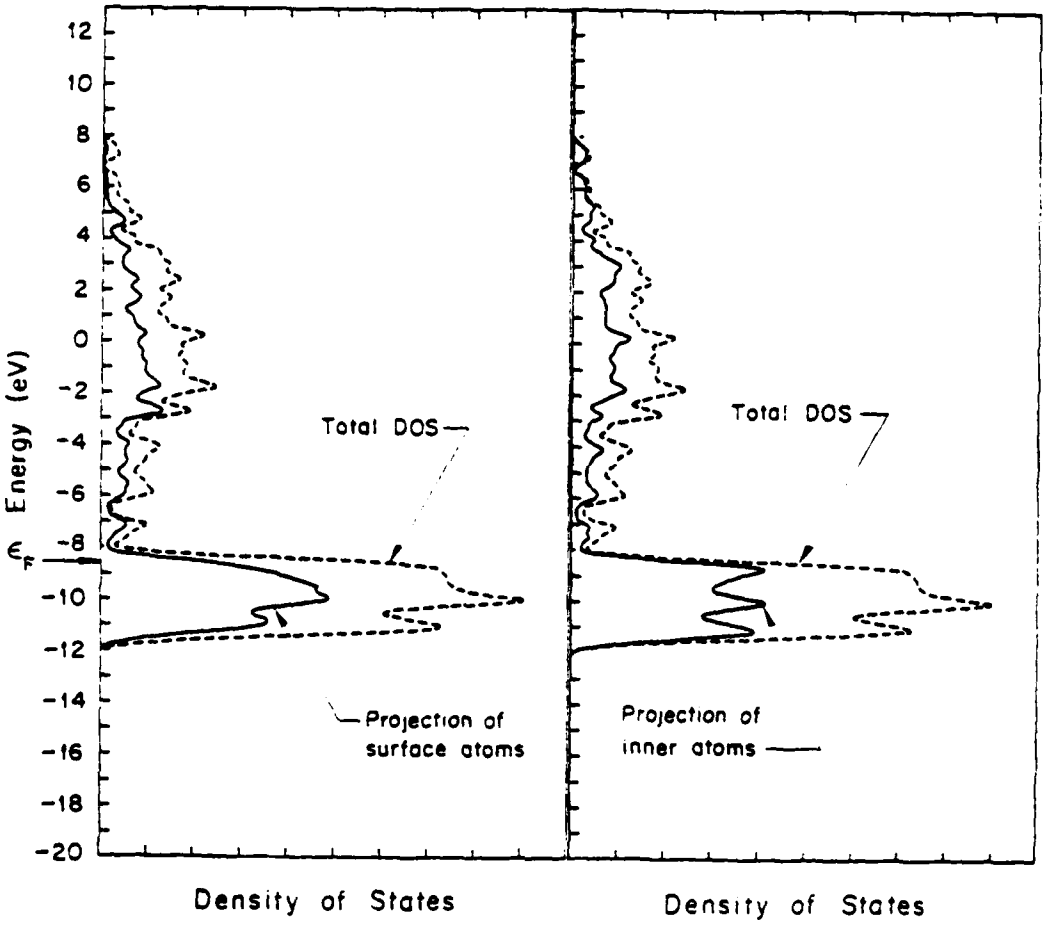

Fig. 12 Those parts of the total density of states of a four-layer Ni (111) slab which are on the surface and inner layers. The dashed line is the total density of states.

33

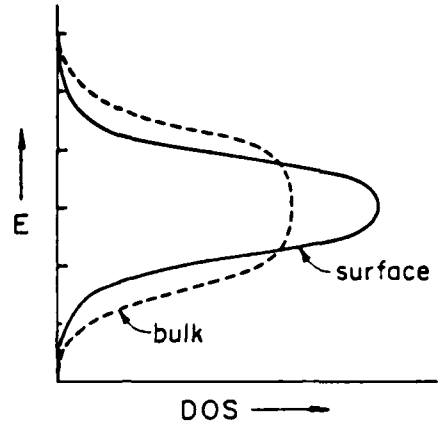

34

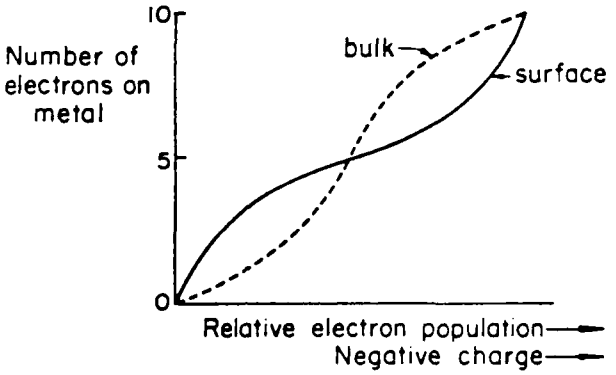

In reality, as one moves across the transition series to provide the variation in electron count, the average energy of a d electron, i.e. the center of gravity of the bands in 33, varies as well. The general lines of the argument remain - at the right side of the transition series surfaces should be negative relative to the bulk, at the left side of the transition series surfaces should be positive. For the specific case of our four layer Ni(111) slab the surface atoms each carry a charge of -0.16, while the inner atoms are +0.16.[7,22]

The above-mentioned crossover in the behavior of the electron density at the surface as a function of electron count has been discussed by others prior to us.[7,23] The reader is referred to the excellent papers of Shustorovich[7] for a general development of the subject.

We are now ready to bring H_2 onto the surface.

H_2 on Ni(111)

We cover both sides of the four layer model film of Ni with a monolayer of H_2, as shown schematically in 35. There is one H_2 per surface Ni, i.e. a total slab stoichiometry $[Ni_4H_4]_\infty$. Each H_2 is "on top" or per-

35

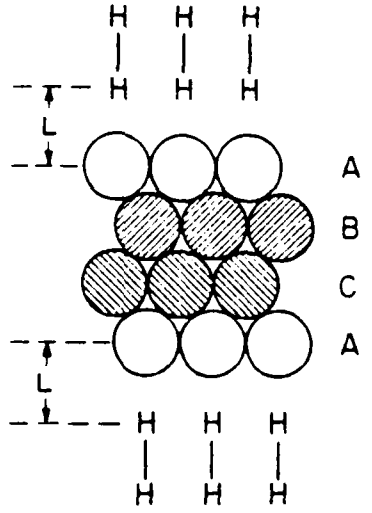

pendicular", above a surface Ni atom.[24] The H-H distance is frozen at 0.74 Å, and the nearest H···Ni distance is varied, L. We are studying here as closely analogous a situation as possible to the perpendicular approach of H_2 to a discrete ML_n complex.

The total density of states for L=3.0, 2.5, 2.0 Å is shown in Figure 13. At 3.0 Å separation we would expect little interaction between substrate and surface, and indeed what we see is two sharp bands for the monolayers of H_2 σ and σ^*, superimposed on the film band structure. Note, however, even here the

Figure 13 here

slight destabilization of the σ^* band relative to the free molecule value. As the H_2 approaches the surface the σ orbital band retains its identity, persisting in its inefficient interaction with the surface. σ_u^*, on the other hand, begins to break up.

The projections of the density of states on σ_u^* (i.e. the fraction of the DOS that is σ_u^*) of Figure 14 clearly show the strong interaction of σ_u^* with the s, p and d bands. At L=2.0 Å some fraction of σ^* (2%) has

Figure 14 here

been mixed into the s, p band, especially around -3 to -5 eV. 75% of the σ^* is pushed up to high energy, > 8 eV. What is happening here is a typical 2 level interaction, 36, except that it is now distributed over the myriad of levels of the $H_2\sigma^*$ and metal s, p bands.

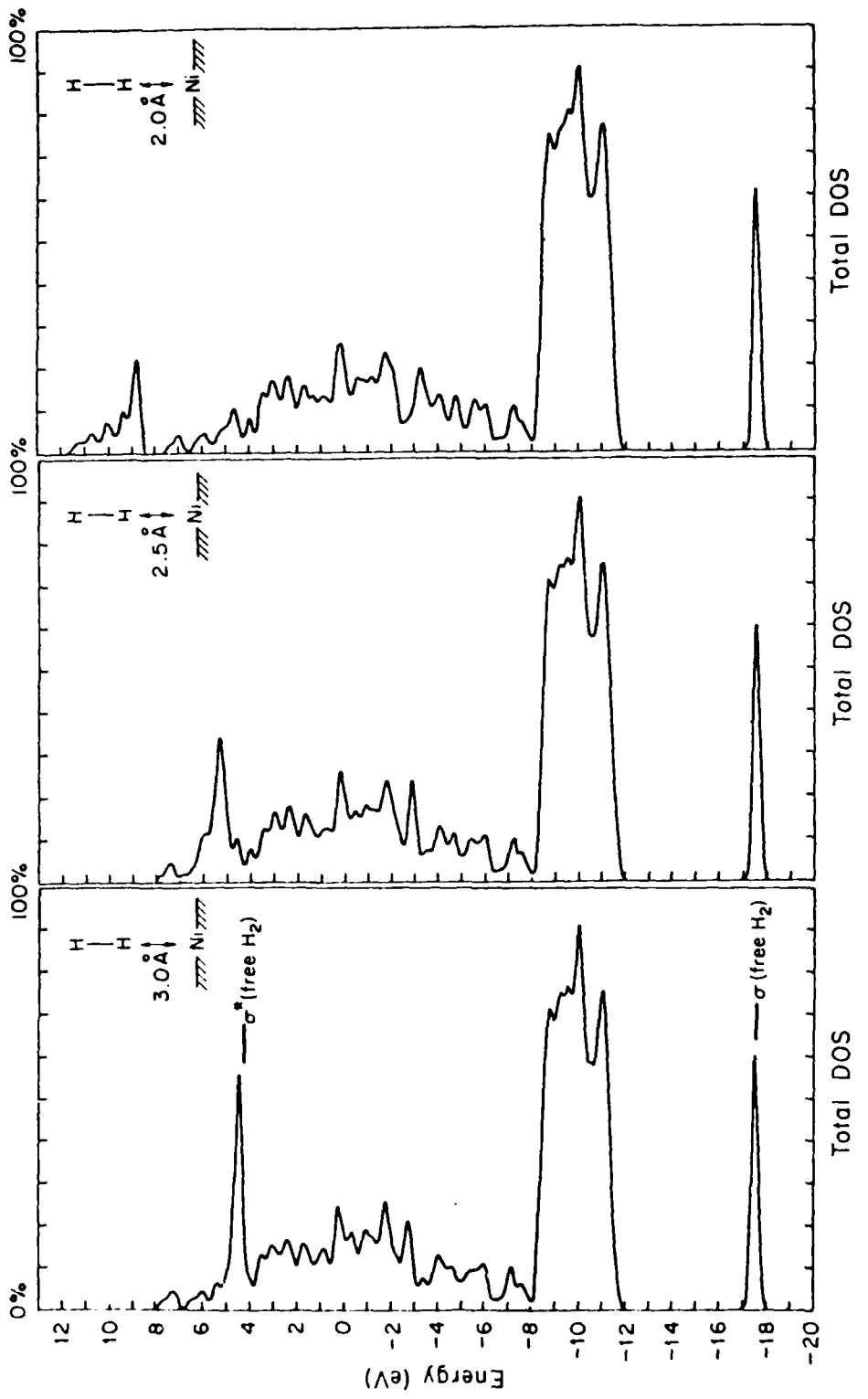

Fig. 13 The total density of states for H_2 approaching a four-layer Ni(111) slab, at L=3.0, 2.5, 2.0 Å. The positions of free H_2 σ and σ* levels are marked on the L=3.0 Å plot.

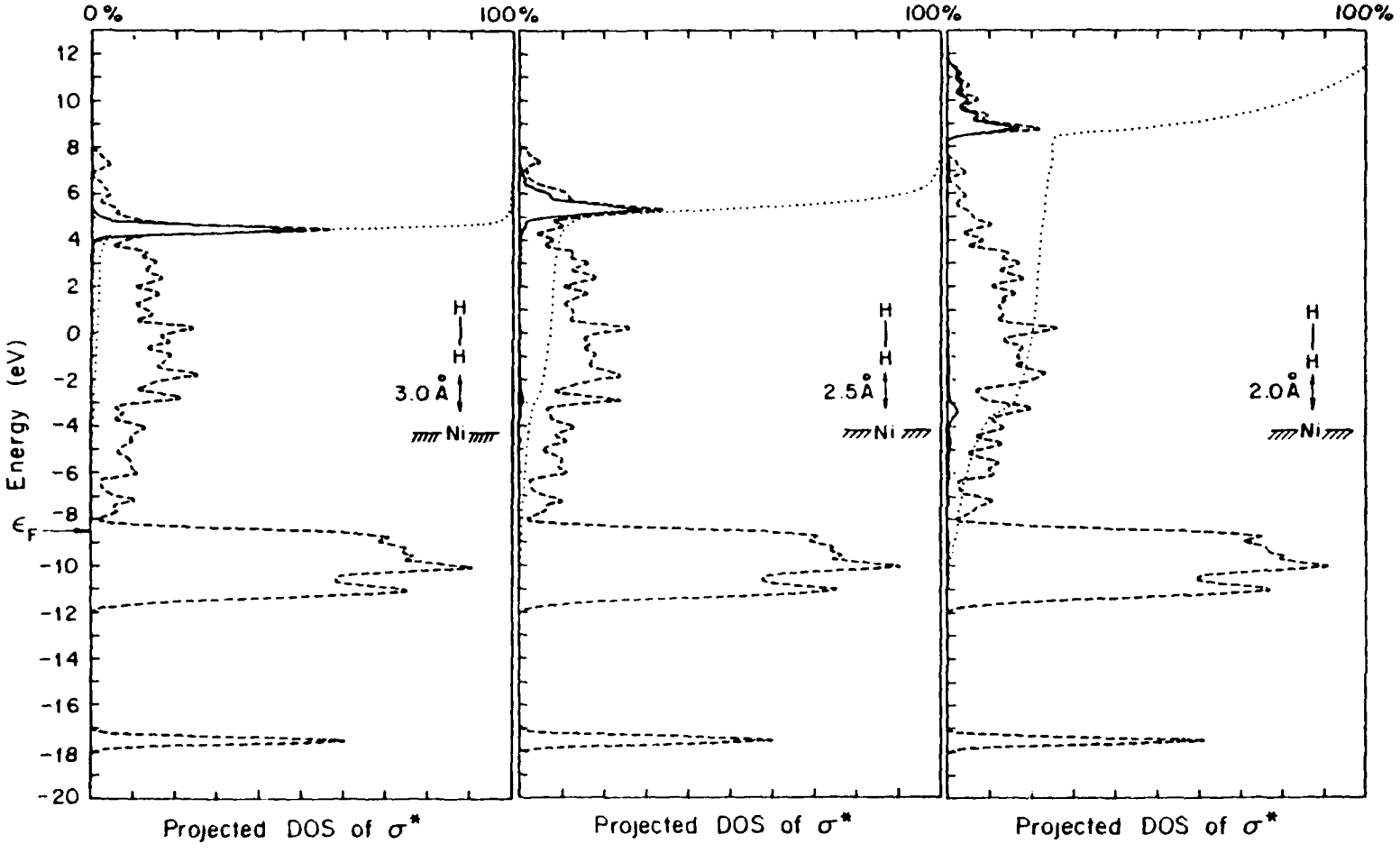

Fig. 14 The part of the total DOS (dashed line) which is in the $H_2\sigma^*$ (solid line) at various approach distances to a Ni (111) surface. The dotted line is the integrated density in σ^* and refers to the top scale.

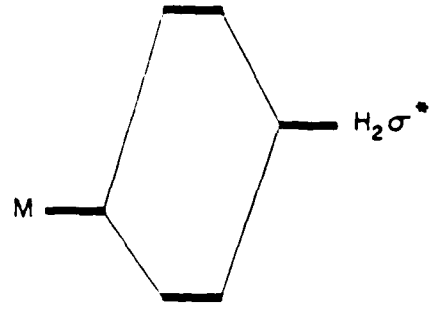

36

There have been a number of theoretical studies of the interaction of H_2 with transition metal surfaces, modelled either by films or by clusters[7,25]. We have mentioned earlier the work of Baetzold, Shustorovich and Muetterties[7], and here refer further to the work of Salem and Leforestier[25a] and of Lundqvist and coworkers[25b]. The former authors stress the importance of interactions with both σ and σ^* of the substrate, much as we will do below. Lundqvist has carried out a thoughtful analysis of metal surface adsorbate interactions. In his model, the H_2 bond breaks because the surface - H_2 resonance cor-

resonance corresponding to σ_u^* falls in energy and is filled as H_2 approaches the surface. We do not get such an effect, but perhaps the analogue in the extended Hückel model is the lower group of states induced by σ^* in the s, p band as seen in Figure 14.

We have shown what happens to the energy levels. What about the bonding? We can look at the COOP curves as a function of L (Figure 15). At large L the H-H bonding is picked up as one sweeps through the σ_g level,

Figure 15 here

and H-H antibonding (more than the bonding!) as one passes through σ_u^*. As one moves the H_2 in these features persist, but now Ni-H bonding enters. Look at L=2.0 Å. There is a little Ni-H bonding as one sweeps through the $H_2\sigma$ bond. Above that, until one enters the main density of σ_u^*, one passes through a region of Ni-H bonding (and mirrored H-H antibonding.)

The sign of these bonding interactions is a vital clue to the role of σ and σ^* in the bonding to the surface. There are two extreme possibilities: (a) σ-metal interaction dominant; (b) σ^*- metal mixing predominating. Each possibility has different consequences for M-H and M-M bonding, as we will now show.

Suppose σ-M mixing were dominant. Then in some localized orbital scheme we would get 37, simple in- and out-of-phase mixings of σ and

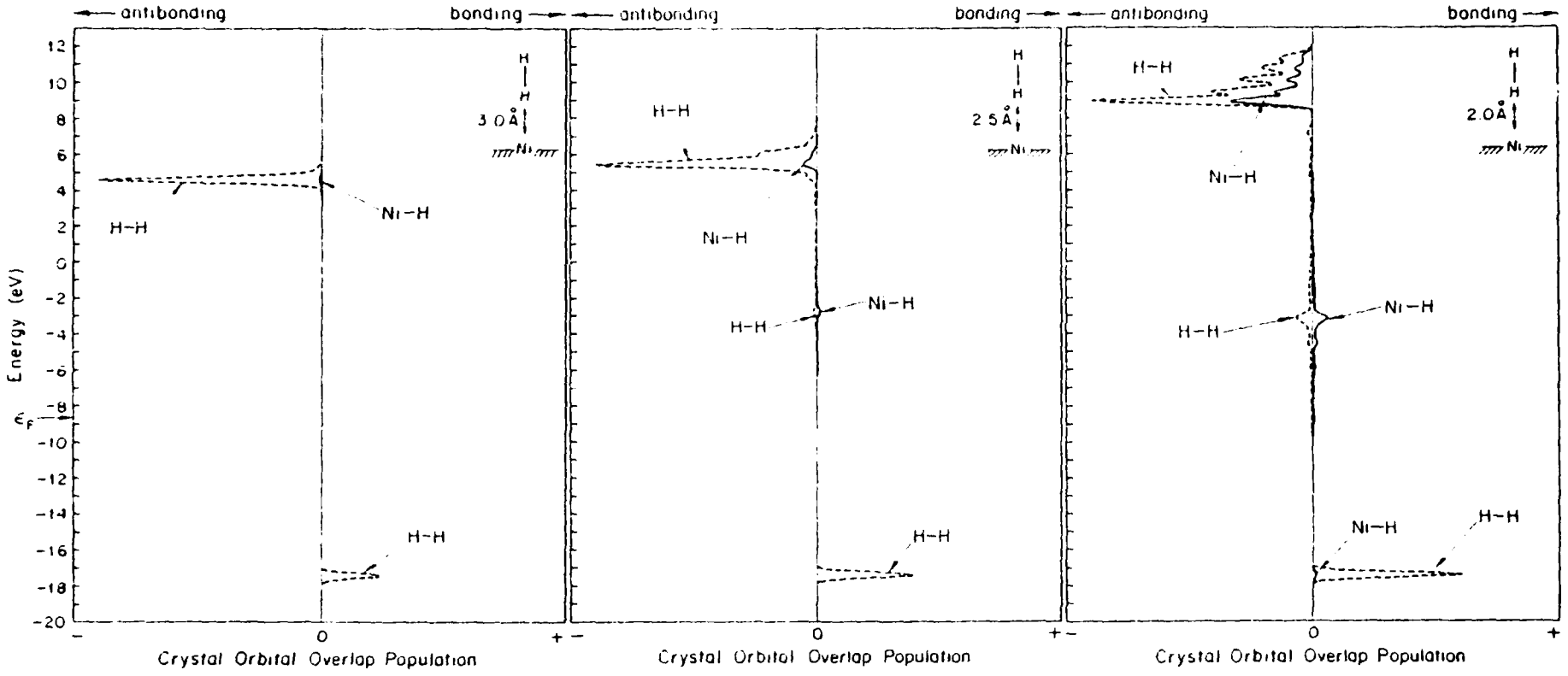

Fig. 15 COOP curves as a function of approach distance of H_2 to a four-layer slab of Ni (111). The solid line is the Ni-H overlap population, the dashed line H-H. The lowest peak is in the region of σ of H_2, the highest where the main density of the σ^* is dispersed.

some appropriate symmetry metal orbital. The resultant COOP curve, when

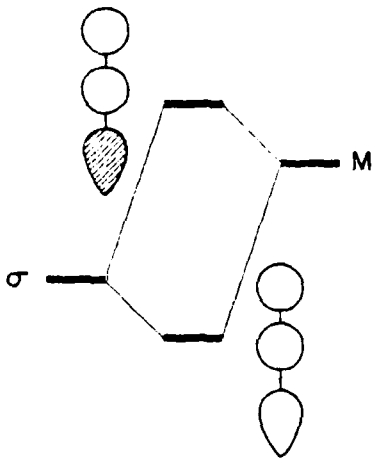

37

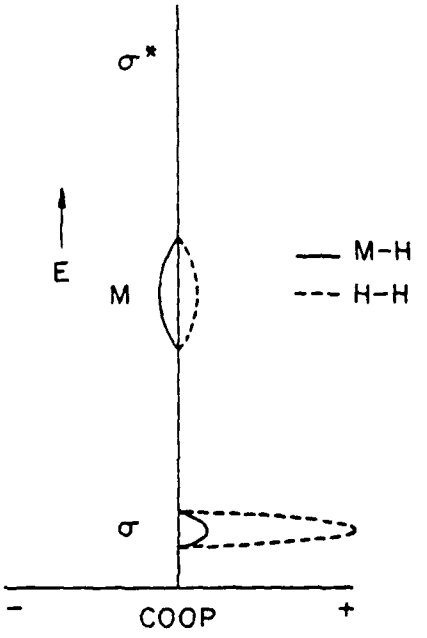

38

this kind of thinking is extended to a band picture, would have the σ band H-H and M-H bonding, whereas the corresponding metal band is still H-H bonding, but M-H antibonding (38).

Suppose instead σ*-M mixing were dominant. Then the localized picture is like 39, and the expected COOP curve 40. Now the lower, primarily metal band, is M-H bonding, but H-H antibonding, through the admixture of σ*. The σ* band itself is both H-H and M-H antibonding.

Reality is the superposition of the two effects. There is no question

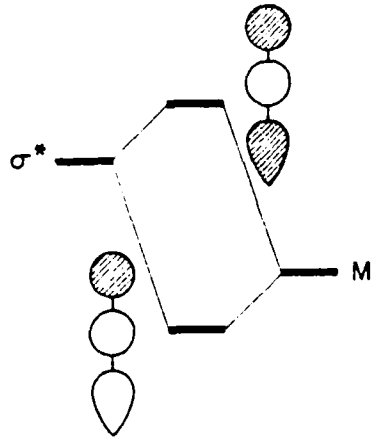

39

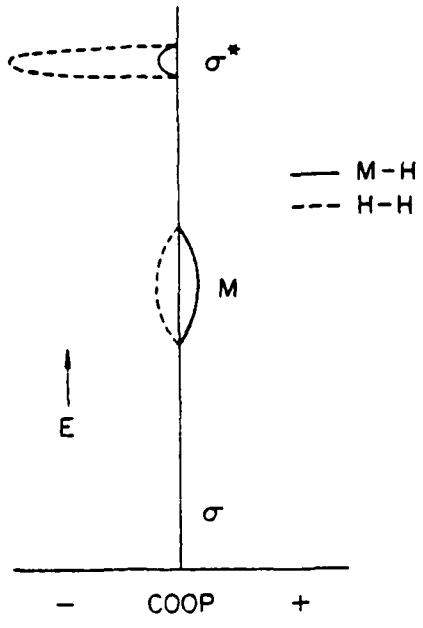

40

what will dominate in the region of the bands derived from H_2 σ_g and σ_u^*. But in the region of the bands derived from the metal the two models give opposite predictions: if σ mixing were dominant over σ^*, the intermediate region should be H-H bonding, M-H antibonding. The reverse should be true if σ^* mixing were dominant. Figure 15 gives a clear answer: In the intermediate region, in the metal bands, the mixing of metal orbitals is

largely in a bonding way with H_2, and H-H bonding is weakened in the same region. Clearly metal surface-hydrogen σ^* mixing is dominant.

Why is this so? There are both energy and overlap reasons. σ_u^* of H_2 lies in the s, p band to begin with. Second, the σ_u^* coefficients are greater, so their overlap with appropriate symmetry surface states is perforce greater than that of σ_g^*.

So far we have looked at the most informative overall picture, independent of electron count, But now it is time to focus our attention on Ni, and what happens below its Fermi level, for its particular electron count.

The overall charge flow and population analysis changes as a function of L are given in Figure 16. Ni-H bonding is turned as L decreases, and

Figure 16 here

H-H bonding is decreased. This is accomplished by populating σ^* of H_2, with relatively minor depopulation of σ. Note the difference between activation in the discrete complex (σ^* not much populated) and on the metal surface (σ^* reasonably populated). The important role of the σ^* in H-H or C-H bonding has been stressed in a number of previous studies,[7,25] especially those of Baetzold, Shustorovich and Muetterties.[7]

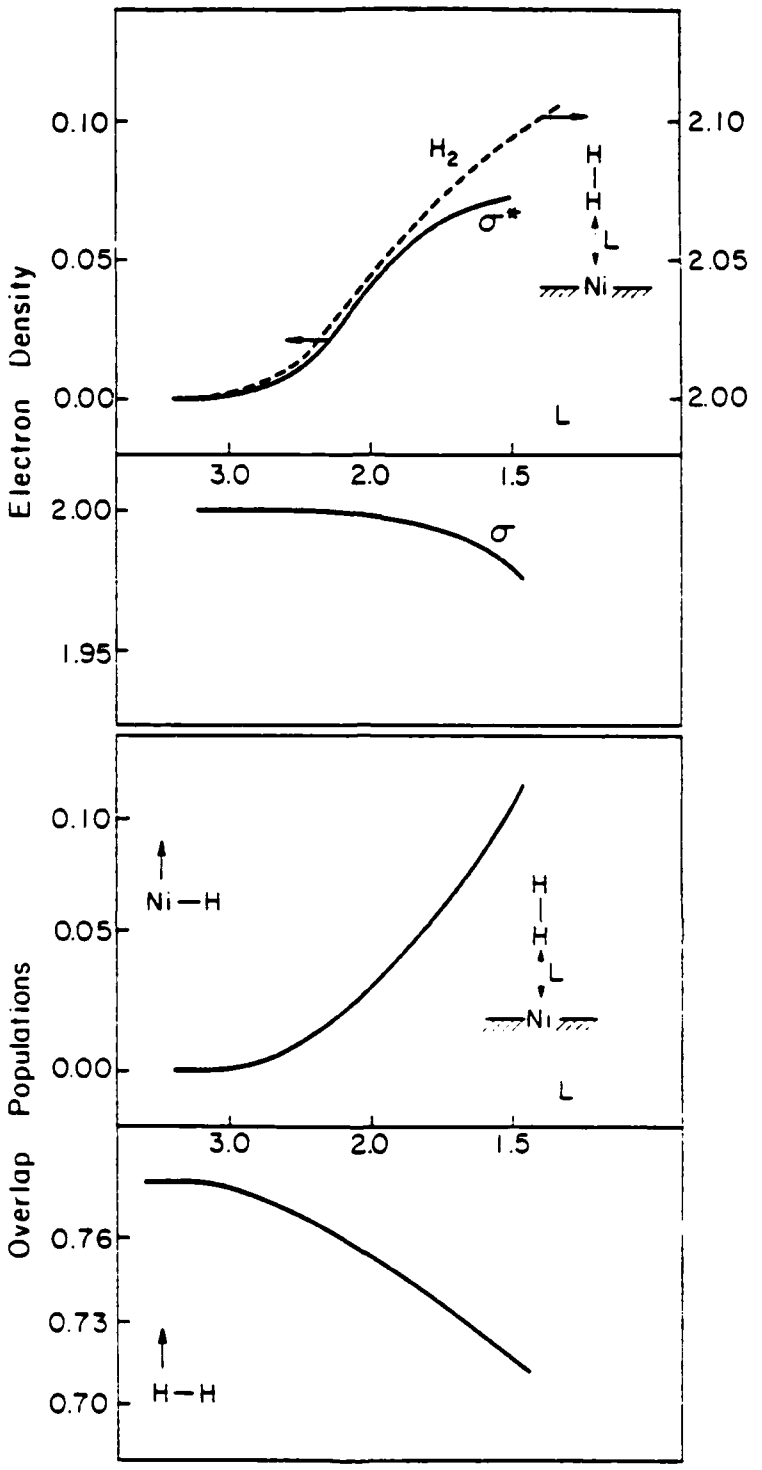

Fig. 16 M-H and H-H overlap populations (bottom) and σ, σ^* and total H_2 densities (top) as a function of L, as H_2 approaches the four-layer slab of Ni (111).

To see how the bond breaking occurs in detail we must apply a microscope to Figures 13-14, and zoom in on the metal d band, -8 to -12 eV. This is where the action takes place. Figure 17 shows the total DOS of the Ni(111) four layer film with H_2 overlayers, L=2.0 Å, in this smaller energy window. The projection of these states on σ is too small to show up, but that of σ^* is clearly visible. It is the integral of this projection up to

Figure 17 here

the Fermi level which gives the 0.044 population of σ^* that may be read off Figure 16.

So σ^* penetrates the d band and is responsible for M-H bonding. But in more detail how does it do it? We can apply a microscope to Figure 15 and zoom in on the COOP in the d band. This is Figure 18.

Figure 18 here

Please note that the scale on the COOP curves is <u>not</u> the same for Figures 18 and 15. The Ni-H and H-H curves mirror each other. Further insight may be obtained by looking at projections of the DOS of the Ni(111) film alone on s, z^2, and xz, yz components of the surface layer, Figure 19. These are the prime orbitals of σ and π local pseudo-symmetry with respect

Figure 19 here

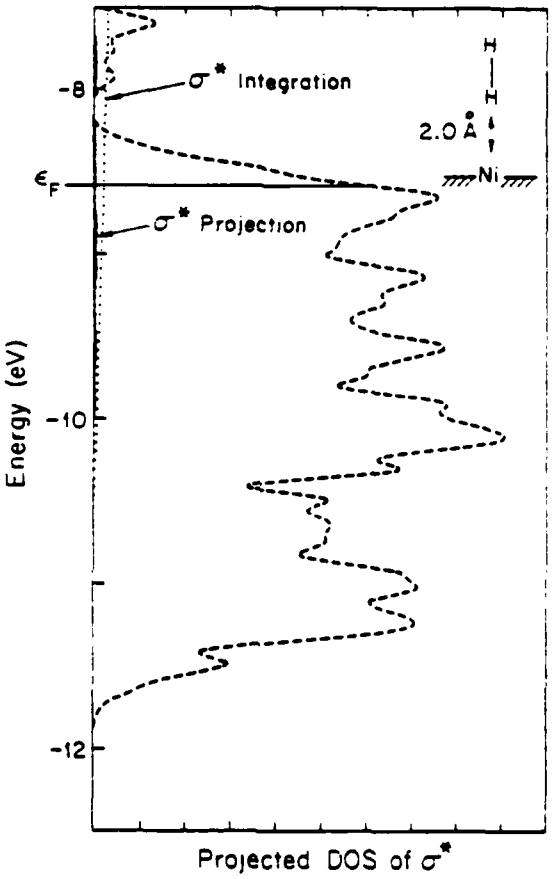

Fig. 17 That part of the total DOS (dashed line) which is the H_2 σ^* (solid line hugging the energy axis). This is at L=2.0 Å, and the energy window shows the Ni (111) d block only. The integrated σ^* population is the dotted line.

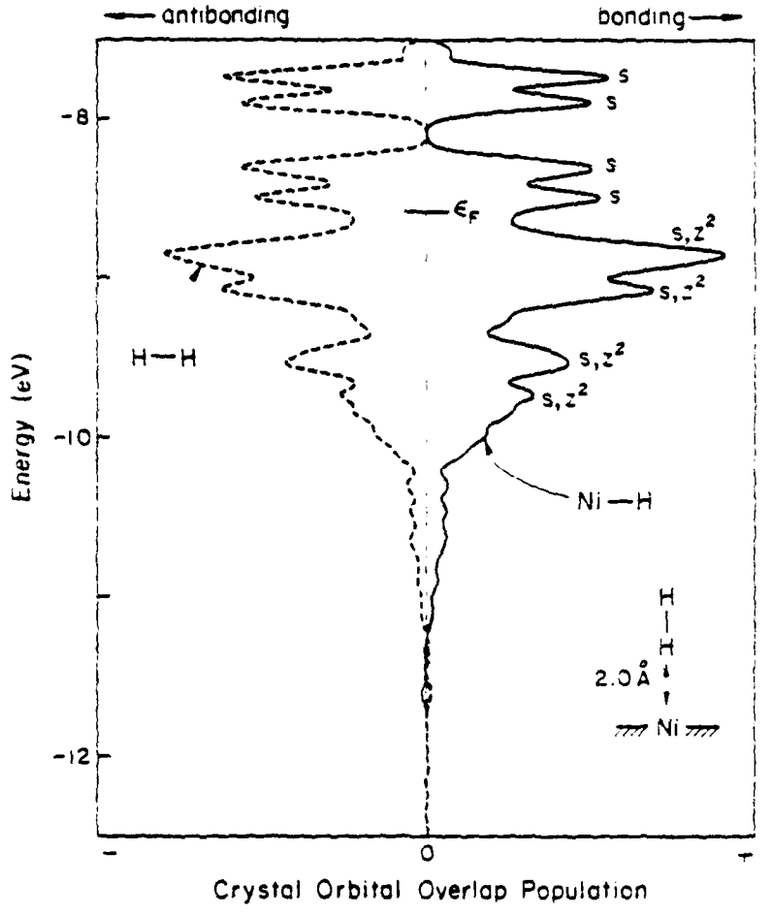

Fig. 18 The COOP curve for Ni-H and H-H bonding in the d block region. H_2 here has approached to L=2.0 A. These peaks in the COOP curve which pick up maxima in the projected DOS curve of surface s and z^2 are marked accordingly.

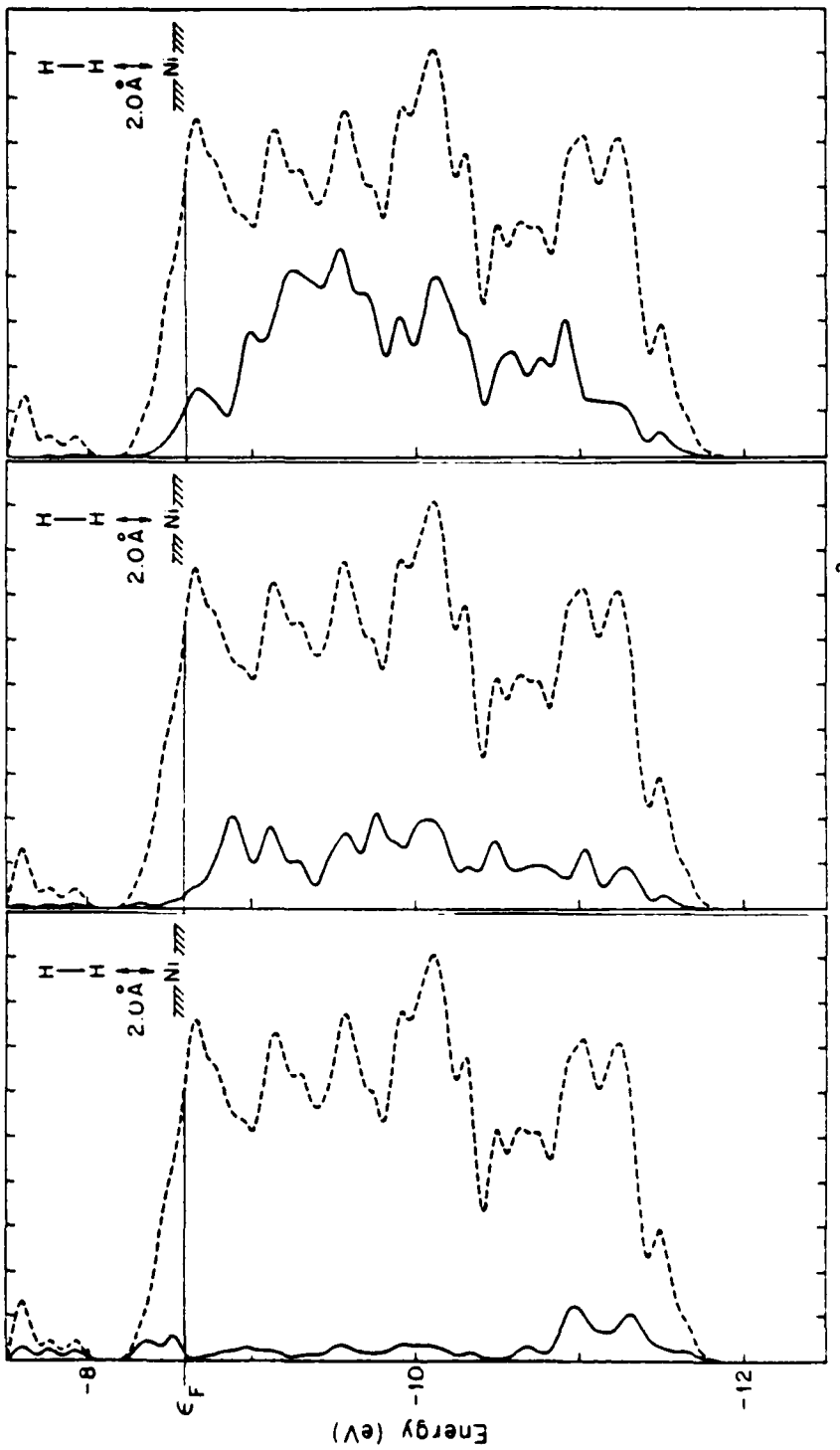

Fig. 19 The parts of the total DOS of a four-layer slab model Ni (111) which are in the surface layers s, z^2 and xz, yz orbitals.

to the impacting H_2.

The features in the COOP curve of Figure 18 clearly pick up corresponding features of the DOS of surface s and/or surface z^2. We have marked the most obvious features in the corresponding curves. The picture is chemically consistent. The surface interacts with the substrate H_2 mainly through $H_2\sigma_u^*$ and surface layer s and z^2 orbitals.

So far we have restricted ourselves to an "on-top", perpendicular approach of H_2 to a Ni surface. Clearly other sites of adsorption and the parallel geometry must be considered. In face we studied further five basic geometries 41 - 45. 41 may be described as three-fold perpendicular, 42 as two-fold, perpendicular, 43 as on-top, parallel, 44 as on a bond, parallel, 45 as across a bond, parallel. For each of these we studied a range of metal-H_2 separations.

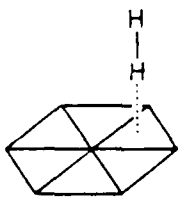

41

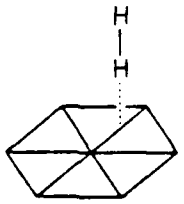

42

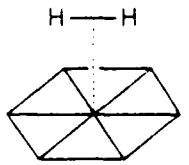

43

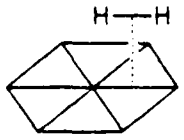

44

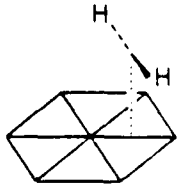

45

It was mentioned earlier that we cannot trust the extended Hückel calculations for the energetics of bond forming or breaking. One would have liked to be able at least to predict reliably relative sites of adsorption, but unfortunately we cannot do that. All of the approach geometries, parallel or perpendicular, give rise to repulsive energy curves. The method overestimates the four-electron repulsive component of the interaction energy. Perhaps one could still hope to argue from the softness or hardness of the repulsion, but we would prefer to abandon the energy criterion, and focus instead on what we know extended Hückel does reasonably well in molecules - the method gives a reasonable estimate of bonding interactions, especially those dependent on orbital symmetry.

We chose to compare the various approaches of H_2 at a similar Ni-H separation of ~2.0 Å. Table 1 gives several calculated quantities for the geometries studied: the Fermi level energy, the change in total energy, M-H and H-H overlap populations, H_2 σ and σ^* populations, the changes in populations of the surface metal layer, both total and classified according to orbital and symmetry type (s, p_σ, p_π, d_σ, d_π, d_δ), and the total change in the inner or bulk-like layer. The changes are relative to the free surface, and in every case the convention is that a negative number implies loss of electron density, or an increasing positive charge.

Table 1 here

Table I. The Consequences of H_2 Approaching Ni(111) in Different Orientations

Geometry	Overlap Populations		H_2 Electron Densities		Ni Surface Layer Change in Electron Density (Total)	Ni Surface Layer Electron Density Changes						Ni Inner Layer Change in Electron Density	ΔE (eV)	ϵ_1 (eV)
	Ni-H	H-H	σ	σ^*		Δs	Δp_σ	Δp_π	Δd_σ	Δd_π	Δd_δ			
Surface and H_2 at Infinite Separation	0	0.782	2.000	0	0	0	0	0	0	0	0	0	0	-8.587
	0.034	0.752	1.997	0.044	-0.049	-0.018	-0.004	+0.000	-0.027	+0.001	+0.001	+0.008	0.060	-8.587
	0.053	0.747	1.993	0.072	-0.121	-0.078	-0.009	-0.011	-0.018	-0.014	+0.011	+0.055	0.328	-8.582
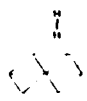	0.047	0.745	1.993	0.065	-0.102	-0.064	-0.009	-0.006	-0.019	-0.011	+0.008	+0.044	0.118	-8.583
	-0.017	0.768	1.985	0.023	-0.114	-0.102	-0.007	+0.004	-0.049	-0.000	+0.038	+0.107	0.452	-8.568
	0.061	0.747	1.987	0.050	-0.180	-0.126	+0.006	-0.018	-0.025	-0.012	+0.045	+0.144	0.434	-8.547
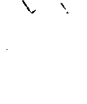	0.007	0.753	1.979	0.041	-0.203	0.176	+0.003	-0.021	-0.024	-0.041	+0.058	+0.183	0.750	-8.538

[a] In cases where there is more than one M-H contact, the entry is for all the Ni-H contacts, to one H_2 molecule, summed.

[b] Electron density of both surface(or inner) layers, summed, relative to layer without H_2. Negative Δn means loss of electron density, or positive character.

[c] Electron densities of specified orbitals in both surface layers, summed, relative to the same orbitals in the uncovered surface layer. Negative numbers mean electron density is lost.

[d] E(geometry)-E(separated H_2 and Ni films). Positive ΔE implies destabilization.

Let us review what happened in the first on-top, perpendicular approach. The Fermi level is raised slightly, the approach is destabilizing or repulsive, M-H forms and H-H begins to weaken. There is minimal effect on σ, but substantial electron transfer to σ^* of H_2. That electron transfer occurs primarily from the surface layer and in the surface primarily from the s and $d_{\sigma}(=z^2)$ orbitals. All other effects are small.

Three-fold perpendicular, 41: In this geometry there is substantial destabilization, yet good M-H bond formation and H-H bond weakening. The COOP curve of Figure 20 shows something new, some features at low energy which indicate interaction with σ in addition to σ^*.

Figure 20 here

What is happening here is that both H_2 σ and σ^* can interact with surface orbitals which are bonding between all 3 metals, as shown schematically in 46. These orbitals are the 3d orbitals at the bottom of the band, and

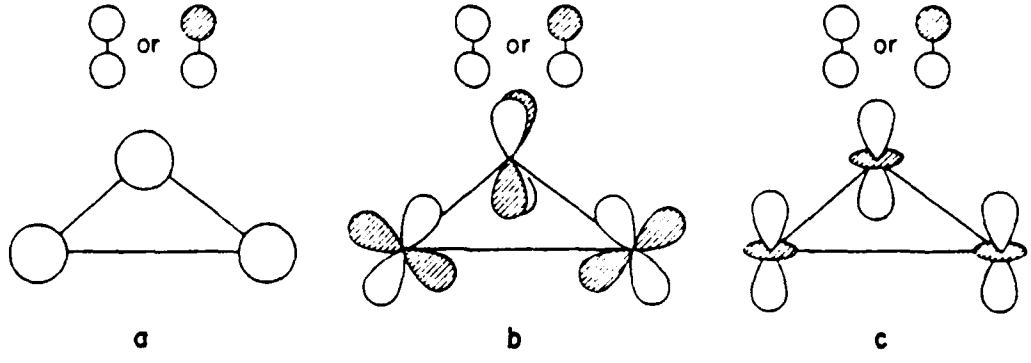

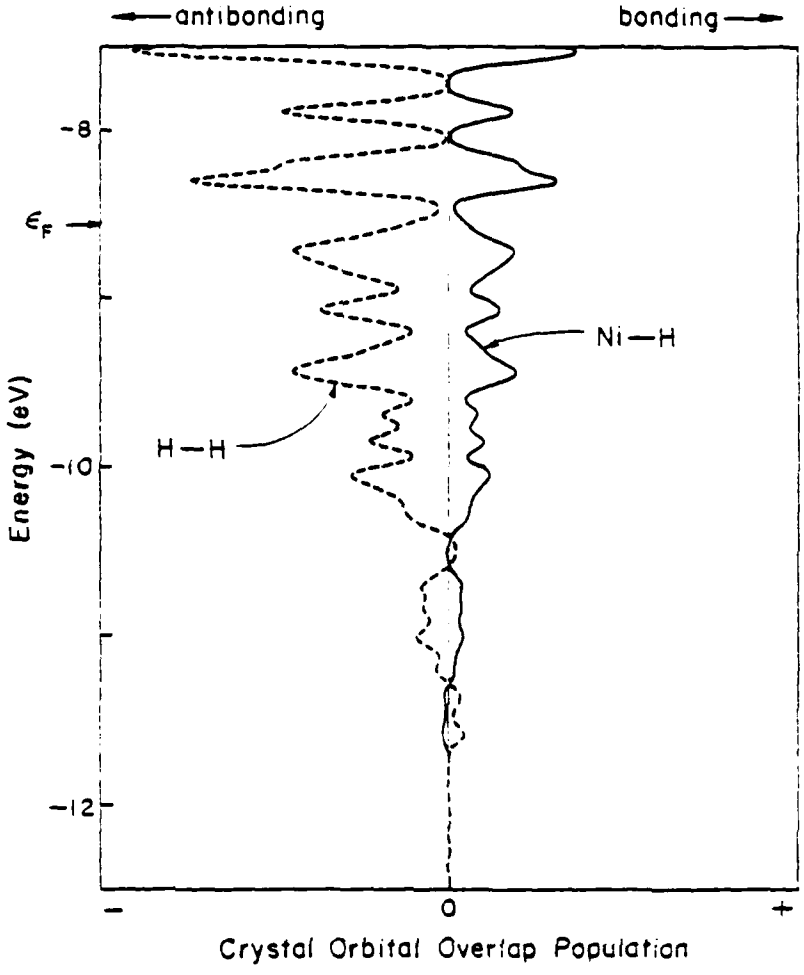

Fig. 20 The COOP curve for Ni-H and H-H bonding when H_2 is perpendicular to the surface, on top of a three-fold hollow site (geometry 47).

most of the s orbitals in the d band, since the latter are the bottom of the s band.[26]

The interaction is strong, because it occurs with three metal atoms instead of one. σ^* still dominates the mixing, but there are signs that σ begins to enter the picture. Note for instance the destabilization, the result of (overestimated) interactions between the surface and σ. Also the Fermi level rises slightly.

One interesting feature which is the result of the stronger interaction is the polarization of the metal by the adsorbate. H_2 gains 0.065 electrons, but the surface layer loses -0.121 electrons. It loses them to H_2, but also to the inner or bulk layer. What is at work here is interaction (4) discussed in an earlier section, a substrate-induced reorganization of electron density. This interaction has also been discussed by Shustorovich.[7] Let us examine this process in some detail.

Suppose that there is some distribution of levels in the band such that some levels are more surface-like than bulk-like. This is shown schematically in 47, where the surface-like levels are marked as dashed lines, the bulk-

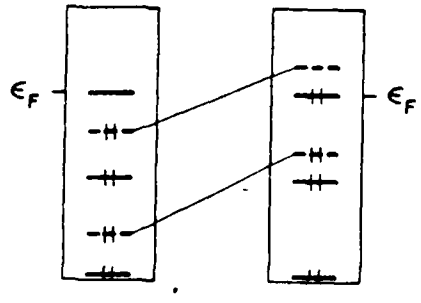

47

like levels as solid lines. If the dominant interaction, as far as energy is concerned, is repulsive (in our case with H_2 σ) then surface-like levels will be pushed up more, some above the Fermi level. The surface layer will be depopulated relative to the bulk. And within the surface those levels primarily involved in interaction (s, d_σ, d_π) will be depopulated relative to those not participating in interaction (for example d_δ).

In the case at hand we see clearly the surface to bulk electron shift, and the increased population of the d_δ, in-plane orbital set. This, in turn, will cause some decrease in metal-metal bonding in the surface, because the newly filled d_δ levels are metal-metal antibonding.

Two-fold, perpendicular, 42: As might have been expected, the results for this geometry are intermediate between the on-top and three-fold sites.

On-top, parallel, 43: The gross indicators of this geometry of approach are disappointing - M-H is not even slightly bonding, and given how good σ^*- M interaction was in the discrete complex it is startling to see so little population of H_2 σ^*. How can this be?

The solid state case of course is much more complicated than the discrete molecular one. For L_5M-H_2 in a parallel geometry the H_2 σ orbital was not allowed, by symmetry, to interact with the same t_{2g} orbital that gained so much when it mixed σ^* into itself. In the extended solid both σ and σ^* of H_2 mix with the metal t_{2g} orbitals everywhere in the interior

of the Brillouin zone. The surface analogue of the π bonding t_{2g} orbital is subjected to both stabilizing and destabilizing forces.

Informative in this respect is the COOP curve of Figure 21 left. The peaks of negative Ni-H (and positive H-H) correspond to peaks in the DOS of s and z^2. It is clear that repulsive interactions with H_2 σ dominate the interaction.

Figure 21 here

But there is a glimmer of hope. In the lower region of the band the peaks of negative H-H overlap population (minima in the Ni-H overlap population) correspond to peaks in the projected DOS of xz (Figure 19). If the σ^* - xz overlap could be increased perhaps this interaction could be magnified. This can be accomplished by bringing H_2 closer to the surface, 48, and by stretching the H_2 bond, 49. Some fragment overlaps which demonstrate

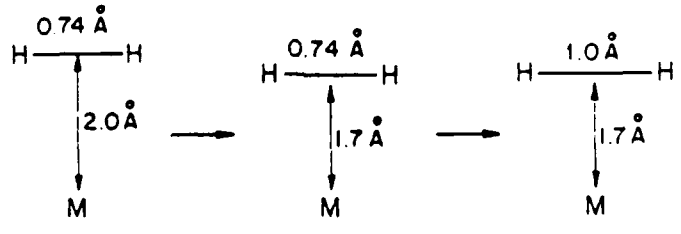

48 49

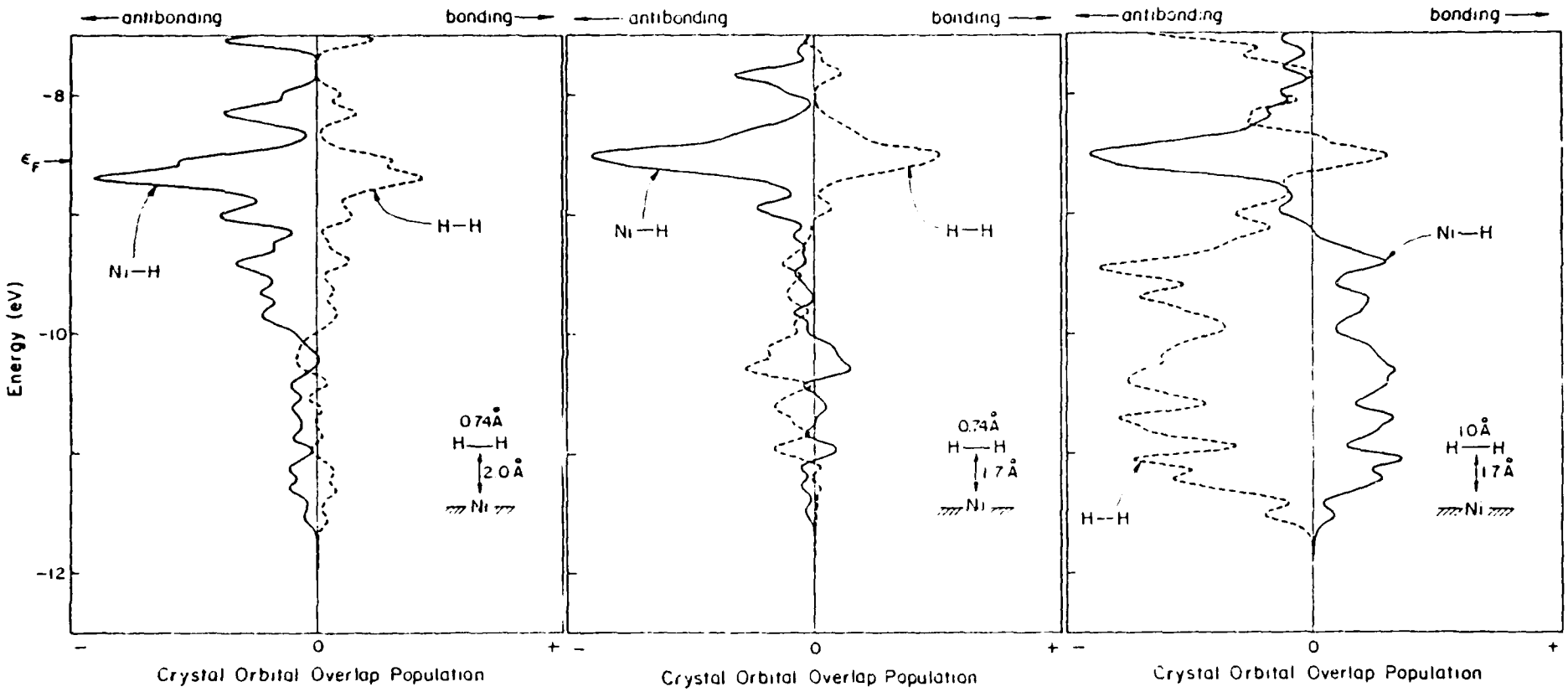

Fig. 21 Evolution of the COOP curve for Ni-H and H-H bonding when H_2 is in the on-top parallel geometry 43 as the molecule approaches the surface and the H-H bond is stretched.

this are shown in Table 2, which also gives population changes as a result of these distance changes.

Table 2 here

Bringing H_2 closer to the metal (48) increases the σ^* - xz overlap greatly. M-H becomes bonding, and σ^* significantly populated. The COOP curve shows increasing improvement in M-H_2 bonding and a growing role for xz. Stretching H_2 makes for still stronger M-H bonding and, of course, substantial population of σ^*. The σ^* - xz interaction dominates the COOP curve.

An interesting feature of the COOP curves is that they indicate stronger M-H_2 bonding for a total electron count of 9, i.e. one less than Ni, for Co. It is this kind of selective catalytic information that we hope to obtain in future studies in this area.

Clearly we have a dissociative process at work. But in the early stages of the reaction it is repulsive, and needs some activation energy. Another parallel approach seems more promising.

On-a-bond, parallel, 44: There is good bonding overall, though repulsive contributions still dominate. Each H_2 interacts significantly with two metal atoms. Characteristic σ mixing, shown in 50, is with z^2 and [illegible] in the lower part of the conduction band, and with s throughout the band. There is much polarization of the metal and electron reorganization within the surface. The H_2 σ^* orbital interacts predominantly with xz and z^2 combinations of

Table 2. Interactions of Several Geometries in the On-Top Parallel Approach of H_2

	$\langle xz \mid \sigma_u^* \rangle$	Overlap Populations M-H	Overlap Populations H-H	Charges σ	Charges σ*
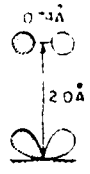	0.072	-0.017	0.768	1.985	0.023
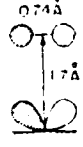	0.125	0.048	0.732	1.974	0.042
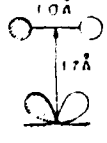	0.130	0.186	0.490	1.934	0.211

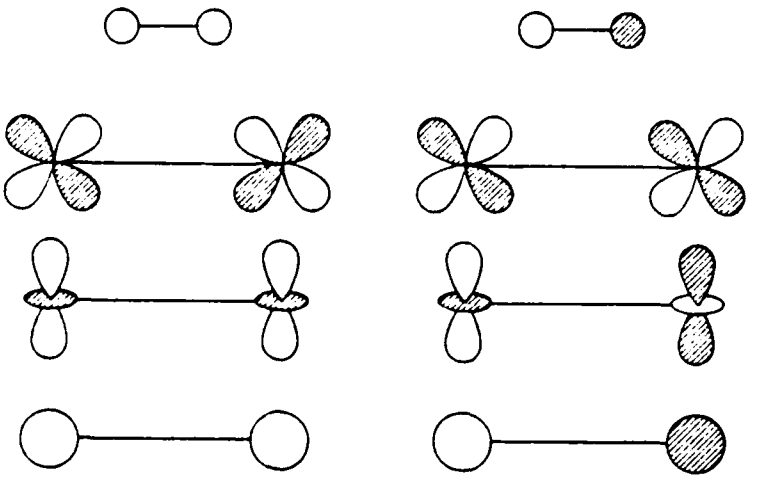

50 51

type 51, in the upper part of the band. The resultant population of σ^* is good, and the Ni-H overlap population the largest in Table 1. Once again a somewhat lower electron count will give better M-H bonding.

The alternative across-a-bond, parallel geometry, 45 shows no special features, though its bonding interactions grow if H-H is stretched.

To summarize: We cannot compute a potential energy surface, but with some detective work through the projected DOS and COOP curves and populations we can trace the origins of the various bonding trends. A significant aspect of this section is our finding of optimum M-H bonding for a parallel geometry in which H_2 is lying over a bond, 44 or 52. This kind of two-metal assisted cleavage of H_2 is not possible in a discrete

mononuclear complex.

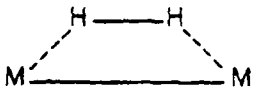

52

The important underlying theme of this analysis is that the interaction of H_2 with a metal surface is qualitatively no different from the similar interaction with the metal center of a discrete molecule. There are important differences in the pacing of involvement of the H_2 σ and σ^* (σ^* is more important in the surface case). But the fundamental aspects of the reaction, which we discussed in the introduction, remain. There is transfer of electrons from H_2 σ, to H_2 σ^*. As a result the H-H bond breaks and M-H bonds form.

Methane on Ni(111)

A 1:1 coverage of a close packed metal surface by methane is not possible, no matter what the approach geometry. The reason for this is excessive steric hindrance between the methanes. We went to a coverage of a third, using the unit cell shown in a solid line in 53, instead of the 1:1 coverage originally used, dashed line. The reduced coverage is $(\sqrt{3} \times \sqrt{3})R30^\circ$.

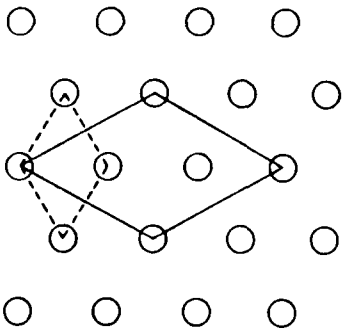

53

The larger unit cell thus brought about forced us to a three layer film in place of the four layer one we had used previously. We also economized by covering only one side of the film.

Several geometries are feasible, 54- 58 among them. The methane molecules, fixed tetrahedral with C-H~ 1:1 Å [27] were placed so that all the closest Ni-H contacts were 2.0 Å. The various approaches are label-

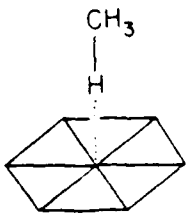

54, 1H on top

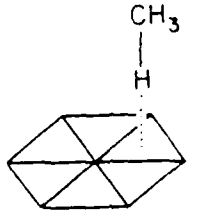

55, 1H three fold

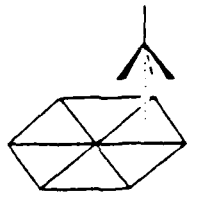

56, 3H

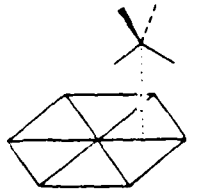

57, 2H along bond

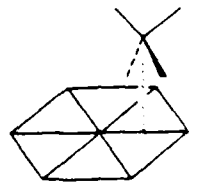

58, 2H across bond

led by the number of hydrogens directed toward the surface, and by a geometrical descriptor. Some calculated quantities, paralleling those we found useful to analyze for adsorbed H_2, are given in Table 3. Among the three $t_2(\sigma)$ orbitals of CH_4, those which are interacting preponderantly with the surface are the ones bearing the largest coefficients on the interacting hydrogen(s).

Table 3 here

These orbitals are shown in 59.[26]

Table 4. The Consequences of Approaching CH_4 to Ni(111) in Different Orientations

Geometry	Overlap Populations		CH_4 Electron Density	Ni Surface Layer Change in Electron Density (total)			Electron Density Changes in Ni Surface Layer[d]				Ni Inner Layer Change in Electron Density		$\Delta E^{e,f}$ (eV)	ε_F (eV)
	Ni-H[a]	C-H[b]	σ	σ^*	z_1	z_2	z_{p_σ}	Δp_π	Δd_σ	Δd_π	Δd_δ			
Surface and CH_4 at Infinite Separation	0		8.0	0	0	0	0	0	0	0	0	0	0	-8.587
	0.037	0.763	7.984	0.036	-0.057	0.040	0.003	-0.001	-0.046	+0.004	+0.020	+0.037	0.154	-8.573
	0.050	0.760	7.974	0.055	-0.081	0.203	-0.016	-0.021	-0.061	+0.012	+0.109	+0.152	0.559	-8.558
	0.067	0.773	7.961	0.062	-0.263	0.263	-0.014	-0.019	-0.136	+0.034	+0.136	+0.240	0.882	-8.555
	0.057	0.769	7.971	0.049	0.168	0.145	-0.009	-0.009	-0.108	+0.022	+0.073	+0.148	0.480	-8.559
	0.078	0.762	7.959	0.093	-0.450	-0.098	+0.003	-0.010	-0.011	-0.028	+0.062	+0.398	1.140	-8.558

[a] In cases where there is more than one Ni-H contact, the entry is for all the Ni-H contacts, towards one CH_4 molecule, summed.

[b] Average of bonds pointing towards surface.

[c] Electron density of surface layer by CH_4 relative to the same layer without CH_4.

[d] Electron densities of specified orbitals in the surface layer atoms in contact with CH_4, relative to those in the uncovered layer.

[e] E(geometry) E(separated CH_4 and Ni films).

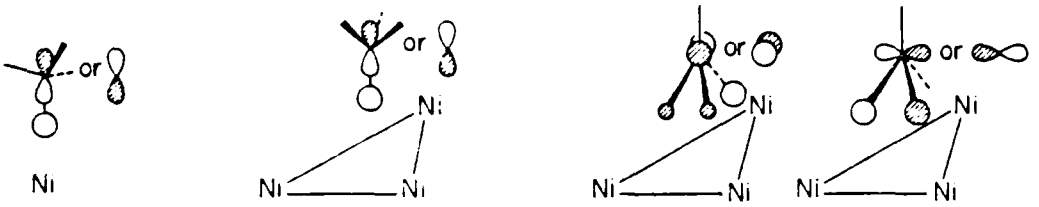

1H, on top 1H, three fold 3H

2H, along bond 2H, across bond

59

Notice that in all cases, σ and σ^* have the same phase relationship on the interacting hydrogen(s) and consequently will interact with the same surface orbitals. The 1H geometries, on-top or over a three-fold site, are remarkably

similar to their H_2 counterparts. There is repulsion, M-H bonding, C-H bond weakening, transfer of electrons from methane σ and into σ^*, loss of electrons from surface s, and $d\sigma$, substantial polarization of the surface. In general there is more mixing with methane C-H σ orbitals. This was expected, for it will be recalled that the CH_4 t_2 is ~2 eV above H_2 σ_g, and thus closer in energy to the metal d block. The stronger interaction with methane σ manifests itself in the greater (relative to H_2) depopulation of σ, and the greater reorganization in the metal (see the population shift to the inner layer and $d\delta$).

As for H_2, 54, CH_4 in the three-fold site, gives more surface-absorbate bonding than 53, because of its larger number of Ni···H contacts.

The 3H and 2H geometries, which have several of these contacts, are excellent for Ni-H bond formation. In 56 and 57, since the H atoms are close to on-top positions, the interacting surface states are s and z^2. 58 gives the larger Ni-H overlap population, in this geometry s surface orbitals are involved but also interactions of type 60 are engendered between σ^* and a piece of the yz band. The geometrical match and overlap are excellent. The culmination of double C-H bond breaking in this geometry would be the formation of surface hydride and methylene.

Geometries in which one Ni atom is in contact with 2 or 3 H atoms have been also studied. In both cases negative Ni - CH_4 overlap population

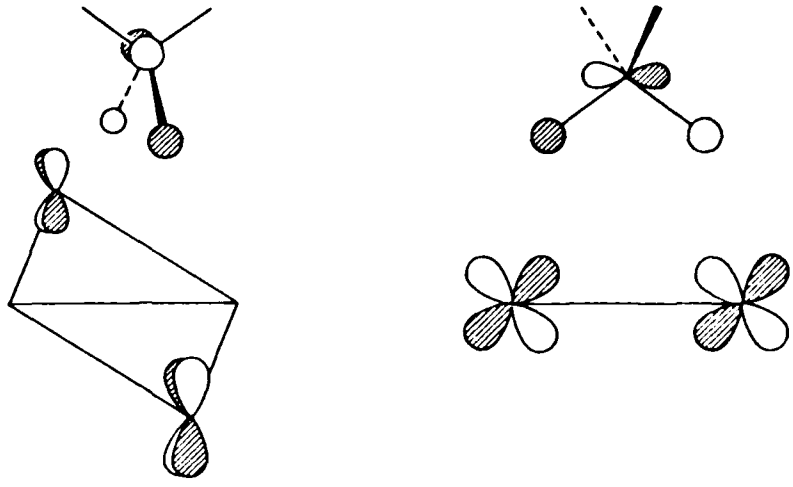

"front" "side"

60

are found, resulting from strong repulsive interactions of type (3). These occur via the H-atoms and also through the C-atom which in these geometries is not far from the Ni atom.

We have mentioned earlier the important recent study of Baetzold[7] on the interaction of hydrocarbons with transition metal films. That work is very much in the same spirit as ours. We are in agreement in the direction of charge transfer between methane and the surface, and the importance of the σ^* orbitals. There is some disagreement between our respective calculations on the preference given to different geometries of approach.

Returning to general considerations, we think that it is interesting that the overlap population corresponding to <u>one</u> interacting hydrogen in <u>58</u> is about equal to the Ni-H overlap population in <u>54</u> and lower than the one

of 55. The C-H overlap population in these three geometries is also about the same. This leads us to think that for cyclic or chain alkanes chemisorption may proceed by a variety of surface - H contacts, the major criterion of stability being the largest possible number of H atoms in contact with the surface that can be produced by matching of the surface and alkane geometries. Recent studies of cyclohexane on Ru(001), where contacts of kind 54 are suggested[6f,m], support this idea.

H_2 and CH_4 on Titanium

The (001) surface of Ti h.c.p. exhibits hexagonal packing very similar to Ni(111): the stacking is of the type ABAB for Ti(001) and ABCABC for Ni(111). The main difference between the two surfaces can be understood from figure 10: Ni and Ti are at each end of a monotonic series. The Fermi level of Ti is ~2 eV higher in energy than the one of Ni. Consequently interactions of type (2) metal acting as donor relative to σ^* orbitals, are expected to be greater with Ti. This is also reinforced by a better overlap of σ^* orbital with surface orbitals, due to the diffuseness of Ti atomic orbitals. On the other hand the bottom of the Ti d band is ~3 eV higher in energy than the one of Ni, consequently repulsions of type (3) are smaller with Ti.

For H_2 dissociation the same geometries (except for 41) as for H_2 on Ni(111) have been studied; the main calculated quantities are summarized in Table 4.

Table 4 here

Qualitatively, there is no big difference between the bonding of H_2 on Ti(001) and on Ni(111). However, except for H_2 on top of a metal atom, considerably larger metal-H overlap populations are obtained, associated with small H-H overlap populations.[28] Clearly, Ti is much more dissoc-

Table 4. Titanium (001) - H_2 Interactions

Structure	Overlap Populations		H_2 Electron Densities	
	Ti - H[a]	H - H	σ	σ*
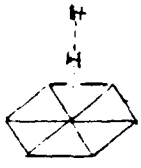	0.026	0.755	1.998	0.041
	0.112	0.682	1.988	0.120
	0.068	0.695	1.993	0.102
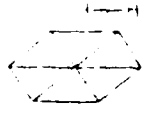	0.420	0.603	1.990	0.211
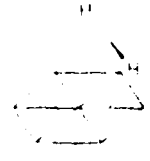	0.238	0.590	1.986	0.231

[a] In cases where there is more than one Ti-H contact, the entry is for all the Ti-H contacts to one H_2 molecule, summed.

iative than Ni. The geometry of type 44 is still the best candidate for a low energy dissociative process.

An approach configuration of type 45 gives much more metal-H bonding with the Ti(001) surface. This is also a consequence of the diffuseness of titanium atomic orbitals: The interaction of σ^* with the nearest metal atom is of δ type, this interaction is weak on Ni(111) but larger on Ti(001), due to better overlap with diffuse yz Ti atomic orbitals. In addition, the interaction with the second nearest metal (situated for both surfaces at ~2,4 - 2.5 Å) is negligible on Ni(111) but important on Ti(001). The total resulting interaction is shown in projection in 61. It involves the bottom of the yz band.

61

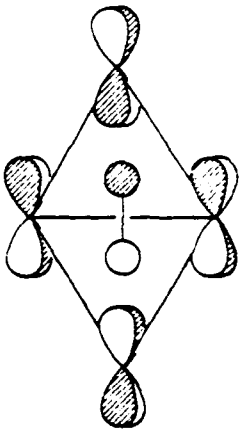

Another typical feature of Ti(001) is that for some geometries, namely 43 and 44, the bulk layer is depopulated. This is the consequence of another variant of interaction (4), the "reverse" of 47, shown in 62.

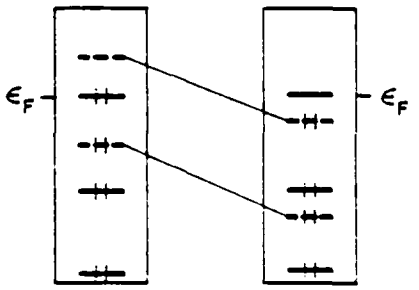

62

Some empty surface states situated close to the Fermi level are, by interaction with σ^*, pushed down below the Fermi level and become populated, taking their electrons from non-interacting (bulk and surface d_δ) filled levels situated near the Fermi energy.

For methane on Ti the results summarized in Table 5 are not qualitatively very different from those concerning CH_4 on Ni(111). Geometries 56 and 58 give the strongest Ni-H bonds. As for H_3, the metal-hydrogen overlap

Table 5 here

population is larger for Ti(001) than for Ni(111) and the H-C overlap population lower. One may expect more dissociative chemisorption of saturated substrates on the surface of metals situated on the left side of the periodic table.

Table 5. Titanium (001) - CH_4 Interactions

Structure	Overlap Populations		CH_4 Electron Densities	
	Ti - H[a]	C-H[b]	σ	σ*
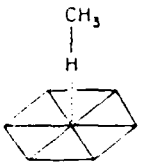	0.045	0.770	7.983	0.024
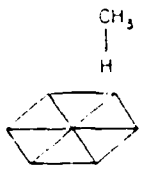	0.115	0.724	7.997	0.124
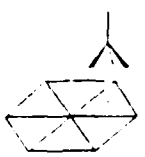	0.167	0.767	7.960	0.089
	0.108	0.767	7.975	0.057
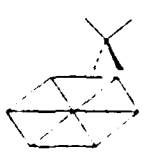	0.157	0.748	7.998	0.169

[a] In cases where there is more than one Ti-H contact, the entry is for all the Ti-H contacts towards one CH_4 molecule, summed.

[b] Average of bonds pointing towards surface.

Concluding Comments

The problems that the extended Hückel method has with bond distances have not deterred us from seeking and obtaining an understanding of the basic features of H-H and C-H activation in discrete transition metal complexes and on two transition metal surfaces.

We have learned much that is specific along the way: why an H_2 adds sideways to a 16 electron ML_5 center, the role of steric problems in CH_4 approaching a metal center, how activation is achieved on d^8CpML fragments, and how it might occur in $d^{10}ML_3$ and ML_2 species, how H_2 interacts initially with a Ni(111) surface, and how that surface differes in electron density from a similar Ti surface, the apparent importance of a two-metal mode of bond cleavage on the surface.

But what is most interesting about our research, we believe, is the demonstration that with proper tools it is possible to illustrate the clear and essential similarity between what happens in a discrete complex and a metal surface. Indeed, how could anything very different happen, for the basic interactions are the same? In the process of breaking an H-H or C-H bond electrons must flow from a σ orbital to the metal, and from the metal to σ^*. The metal-H bond forms at the same time. To be sure there are differences in the pacing of these electron transfers. In transition metal

complexes coordinative unsaturation is essential, and with it the initial stages of reaction are dominated by $\sigma \rightarrow M$ electron transfer. But for Ni(111) the surface is electron rich, the Fermi level is higher than for a molecule, and it is electron transfer from $M \rightarrow \sigma^*$ that dominates the early stages of the reaction.

The analytical tools we use in this paper are a density of states analysis, the projections of that density of states on various atoms and orbitals - very similar to a gross atomic populations for a discrete complex. We introduce an immensely useful new indicator - the crystal orbital overlap populations or COOP curves (technically the overlap population weighted density of states). This is the solid state analogue of a Mulliken overlap population and allows a limpid analysis of bond forming and breaking processes. These tools, along with one we did not use in this paper, the extended structure analogue of Walsh diagrams, give chemists a language for understanding solid state structure and reactivity.

Acknowledgment: The initial stages of this research were carried out by E. D. Jemmis and we thank him for his contribution. We are grateful to Sunil Wijeyesekera, Cyrus Umrigar, John Wilkins, Miklos Kertesz and Bengt Lundqvist for extensive discussions and to Roger Baetzold, Earl Muetterties and Evgeny Shustorovich for communication of results prior to publication. Our drawings were masterfully executed by Jane Jorgensen and Elisabeth Fields, and the typing by Eleanor Stolz. The permanent address of Jean-Yves Saillard is at the Laboratoire de Cristallochimie of the University of Rennes, Rennes, France and his stay at Cornell was made possible by a grant from NATO and by the cooperation of the CNRS. Our research was generously supported by the National Science Foundation through grant CHE 7828048 and by the Office of Naval Research.

Appendix 1. Extended Hückel and Geometrical Parameters.

Molecular Calculations. Extended Hückel parameters for all atoms used are listed on Table 6. Idealized geometries were assumed and standard band lengths and bond angles were used. In the ML_n(n=2-5) fragments, all

Table 6 here

LML bond angles were 180° and 90°. The CpRhCo fragment was bent with the angle (CC)(Rh)(Centroid of Cp) equal to the ideal value of 125.3°; the Rh - centroid distance being 1.85 Å. In the $Rh(C_2H_6)^-$ fragment the Rh - centroid distance was 1.82 Å. All HCH angles were assumed to be 109.47°. The following standard bond distances were used: M - CC = 1.90 Å; C-C = 1.15 Å; Rh - CH_3 = 1.95 Å; Rh - H = 1.60 Å; Rh - P = 2.30 Å; Rh - Cl = 2.30 Å; C(Cp) - C(Cp) = 1.43 Å; C (benz) - C(benz) = 1.41 Å; C-H = 1.09 Å; H-H = 0.74 Å. The geometries of 17 (L = CO; R=R´=H) and 23 were constructed from idealization of experimental structures[5a,d] using bond distances given above.

Bulk and Surface Calculations. All the calculations were of the tight binding extended Hückel type. The same parameters as for molecular calculations (Table 6) have been used for C and H.

The H_{ii}'s of the transition metals from Ti to Ni have been determined by charge iteration on bulk metals, assuming the charge dependence of metal

Table 6. Extended Hückel Parameters Used in Molecular Calculations

Orbital		H_{ii} (eV)	ζ_1	ζ_2	C_1[a]	C_2[a]
Cr	4s	-8.66	1.70			
	4p	-5.24	1.70			
	3d	-11.20	4.95	1.60	0.4876	0.7205
Fe	4s	-9.10	1.90			
	4p	-5.32	1.90			
	3d	-12.60	5.35	2.00	0.5505	0.6260
Rh	5s	-8.09	2.135			
	5p	-4.57	2.100			
	4d	-12.50	4.29	1.97	0.5807	0.5685
P	3s	-18.60	1.60			
	3p	-14.00	1.60			
Cℓ	3s	-30.00	2.033			
	3p	-15.00	2.033			
C	2s	-21.40	1.625			
	2p	-11.40	1.625			
O	2s	-32.30	2.275			
	2p	-14.80	2.275			
H	1s	-13.60	1.30			

[a] Contraction coefficients used in the double ζ expansion

AD-A136 468 C-H AND H-H ACTIVATION IN TRANSITION METAL COMPLEXES AND ON SURFACES(U) CORNELL UNIV ITHACA NY DEPT OF CHEMISTRY J Y SAILLARD ET AL. 1983 TR-1

UNCLASSIFIED N00014-82-K-0576 F/G 7/4 NL

END

DATE FILMED

1-84

DTIC

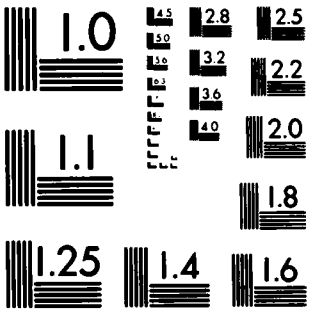

MICROCOPY RESOLUTION TEST CHART
NATIONAL BUREAU OF STANDARDS 1963-A

H_{ii}'s given by Gray's eguations[29]. The A, B and C iteration parameters were taken from Reference 30. Experimental h.c.p, f.c.c. and b.c.c. structures were used[31] except for Mn for which a b.c.c. structure was assumed with a lattice parameter determined by averaging those of Cr and Fe.

The extended Hückel parameters for Ti to Ni are listed on Table 7. Note that they are substantially higher in energy than the same parameters in discrete molecular complexes.

Table 7 here

Calculations of H_2 on Ni and Ti were made assuming a two dimensional slab of metals, four layers thick, with a 1 x 1 coverage on both sides of the slab. Calculations with H_2 on one side give very similar results. Interactions between H_2's have been dropped to simulate a low coverage. The repeating unit cell contains four Ni atoms and two H_2 molecules. A 14 k point set[32] was used in hexagonal symmetry; for lower symmetries, special points set were generated by symmetry reduction of this hexagonal set.

Calculations of CH_4 on Ni and Ti were made with a slab of three metal layers with a $(\sqrt{3} \times \sqrt{3})R30^\circ$ coverage of CH_4 on one side of the slab only. The repeating unit cell contains nine Ni atoms and one CH_4 molecule. A 5 k point[32] set was used in hexagonal symmetry, from which

Table 7. Extended Hückel Parameters Used in Metal Bulk and Surface Calculations.

Orbital		H_{ii}(eV)	ζ_1	ζ_a	C_1[a]	C_a[a]
Ti	4s	-6.3	1.50			
	4p	-3.2	1.50			
	3d	-5.9	4.55	1.40	0.4206	0.7839
V	4s	-6.7	1.60			
	4p	-3.4	1.60			
	3d	-6.7	4.75	1.50	0.4560	0.7520
Cr	4s	-7.3	1.70			
	4p	-3.6	1.70			
	3d	-7.9	4.95	1.60	0.4876	0.7205
Mn	4s	-7.5	1.80			
	4p	-3.8	1.80			
	3d	-8.7	5.15	1.70	0.5140	0.6930
Fe	4s	-7.6	1.90			
	4p	-3.8	1.90			
	3d	-9.2	5.35	1.80	0.5366	0.6678
Co	4s	-7.8	2.00			
	4p	-3.8	2.00			
	3d	-9.7	5.55	1.90	0.5550	0.6678
Ni	4s	-7.8	2.1			
	4p	-3.7	2.1			
	3d	-9.9	5.75	2.00	0.5683	0.6292

[a]Contraction coefficients used in double ζ expansion.

special sets were obtained by symmetry reduction for lower symmetries.

In all calculations the H-H distance is 0.74 Å (unless otherwise specified). The C-H distances were set to 1.1 Å if they were interacting with the surface, if not they were set to 1.09 Å. HCH angles were 109.47°. The Ni-Ni and Ti-Ti distances are taken from Reference 31.

Appendix 2. The Film or Slab Model for Surfaces.

In order to determine the best compromise between time of computation and accuracy of the model, a study of the dependence of surface electronic structure on slab thickness was undertaken. In Table 8 are listed several computed quantities for Ni(111) slabs made up of different numbers of layers.

Table 8 here

These were carried out using a hexagonal 30 k point set[32]. Reasonable convergence is reached for a slab of four layers. Electron densities of the middle layer are not very different from those calculated for three dimensional bulk nickel (using a 110 k point set); the major difference is in the 3d population, due to the negative polarization of the surface layer described in the text.

The overlap population inside the slab is close to the one obtained for bulk Ni. That the Ni-Ni overlap population is largest on the surface may be explained by narrowing of the surface 3d band as shown in 33: Compared to the corresponding inner slab states, the bonding surface states are less bonding and the antibonding states are less antibonding. For nickel almost all the antibonding d levels are filled. As an antibonding level is in fact more antibonding than the corresponding bonding level is bonding, the loss

of antibonding character dominates on the surface, causing the increased Ni-Ni overlap population.

We also have observed that for the four layer slab good convergence is reached for the projected DOS of the surface layer and of the middle layer. Comparison of Figures 10 and 12 shows that the projected DOS of the inner layer of a four layer thick slab resembles the total DOS of the three dimensional bulk Ni.

Calculations of various geometries of H_a on slabs of 3 and 4 layers show that, even if computed electron densities and overlap populations are slightly different, the general trend obtained for a four layer slab is conserved for a three layer slab.

Table 8. The Effect of Slab Thickness on Models for Ni(111)

Number of Layers	Layer No.	Electron Densities				Overlap Populations Between Neighbors		ϵ_F
		Total	s	p	d	On Surface	inside slab (averaged)	(eV)
1	1	10.00	0.66	0.14	9.20	0.171		-9.04
2	1	10.00	0.58	0.19	9.23	0.131	0.109	-8.71
3	1(surface)	10.10	0.63	0.20	9.27	0.134	0.112	-8.59
	2(middle)	9.79	0.60	0.24	8.95			
4	1(surface)	10.16	0.63	0.20	9.33	0.132	0.110	-8.56
	2(middle)	9.84	0.61	0.24	9.00			
5	1(surface)	10.21	0.63	0.20	9.38	0.130	0.110	-8.56
	2	9.89	0.61	0.24	9.04			
	3(middle)	9.80	0.62	0.23	8.95			
3 D Bulk	Ni	10.00	0.62	0.24	9.15	0.107		-8.47

References

1. See for example: James, B.R. "Homogeneous Hydrogenation", John Wiley & Son, Inc., New York, 1973 and references therein.

2. Kubas, G. J.; Ryan, R. R.; Swanson, B. I.; Vergamini, P. J.; Wasserman, H. J. J. Am. Chem. Soc. 1983, 105, ; Kubas, G. J.; Ryan, R. R.; Vergamini, P. J.; Wasserman, H. 185th ACS National Meeting, Seattle, March 1983. Abstract INOR 0229 and: Chem. and Eng. News 1983, 20, March 28, p. 4. Another possible case of this type with a d^6ML_3 fragment is $RHCl(H)_2(P(t\text{-}Bu)_3)_2$. Yoshida, T.; Otsuka, S.; Matsumoto, M.; Nakatsu, K. Inorg. Chim Acta 1978, 29, 157-159.

3. (a) Parshall, G.W.;"Catalysis", Kemball, C.; ed. Chem.Soc.Spec.Period.Rpt.1977, 1, 335-369. Webster, D.E. Adv. Organomet. Chem. 1977, 15, 147-189.

   (b) Muetterties, E.L. Chem.Soc.Rev. 1982, 11, 283-320.

4. (a) Janowicz, A. H.; Bergman, R. G. J. Am. Chem. Soc. 1982, 104, 352-354.

   (b) Jones, W. D.; Feher, F. J. J. Am. Chem. Soc. 1982, 104, 4240-4242.

   (c) Hoyano, J. K.; Graham, W. A. G. J. Am. Chem. Soc. 1982, 104, 3723-3725.

   (d) Shilov, A. E.; Shteinman, A. A. Coord. Chem. Rev. 1977, 24, 97-144; Kinetika i Kataliz 1977, 18, 1129-1145.

   (e) Baudry, D.; Ephiritikhine, M.; Felkin, H. J. Chem. Soc. Chem. Commun. 1980, 1243-1244; 1982, 606-607.

   (f) Crabtree, R. H.; Mihelcic, J. M.; Quirk, J. M. J. Am. Chem. Soc. 1979, 101, 7738-3340. Crabtree, R. H.; Mellea, M. F.; Mihelcic, J. M.; Quirk, J. M. J. Am. Chem. Soc. 1982, 104, 107-113.

   (g) Tulip, T. H.; Thorn, D. L. J. Am. Chem. Soc. 1981, 103, 2448-2450.

   (h) C—H activation has been shown also with organolanthanides and organo-actinide compounds: Watson, P.L. J.Chem.Soc. Chem.Commun. 1983, 176-177. Watson, P. L. J. Am.Chem.Soc. in press. Bruno, J. W.; Marks, T. J.; Day, V. W. J.Amer.Chem.Soc. 1982, 104, 7357-7360. Simpson, S. J.; Turner, H. W.; Andersen, R. A. J.Am.Chem.Soc. 1979, 101, 7728-7729.

References

Nizova, G. V.; Krevor, J.V.Z.; Kitaigorodskii, A.N.; Shul'pin, G. D. Izv.Akad.Nauk.USSR 1982, 12, 2805-2808.

(i) Billups, W. E.; Konarski, M. M.; Hauge, R. H.; Margrave, J. L. J. Am. Chem. Soc. 1980, 102, 7394-7396. Ozin, G. A.; McIntosh, D. F.; Mitchell, S. A. J. Am.Chem. Soc. 1981, 103, 1574-1575. Ozin, G. A.; McCaffrey, J. Am. Chem. Soc. 1982, 104, 7351-7352. Klabunde, J. J.; Tanaka, Y. J. Am. Chem. Soc. 1983, 105, 3544- 3546.

5. (a) For a review on CH— Transition metal bonds see: Brookhart, M.; Green, M.L.H. J. Organometal.Chem. 1983, 250, 395-408.

(b) Otsuka, S.; Yoshida, T.; Matsumoto, M.; Nakatsu, K. J. Am. Chem. Soc. 1976, 98, 5850-5858.

(c) Yared, Y. W.; Miles, S. L.; Bau, R.; Reed, C. A. J. Am. Chem. Soc. 1977, 99. 7076-7078.

(d) Roe, D. M.; Bailey, P. M.; Moseley, K.; Maitlis, P. M. J. Chem. Soc. Chem. Commun. 1973, 1273-1274.

(e) Mann, B. E.; Bailey, P. M.; Maitlis, P. M. J. Am. Chem. Soc. 1975, 97, 1275-1276.

(f) Echols, H. M.; Dennis, D. Acta Cryst. 1976, B30, 2173-2176.

(g) Echols, H. M.; Dennis, D. Acta Cryst. 1975, B32, 1627-1630.

(h) Van Der Poel, H.; van Koten, G.; Vrieze, K. Inorg. Chem. 1980, 19, 1145-1151.

(i) Postel, M.; Pfeffer, M.; Riess, J. G. J. Am. Chem. Soc. 1977, 5623-5627.

(j) Dehand, J.; Fisher, J.; Pfeffer, M.; Mitschler, A.; Zinzius, M. Inorg. Chem. 1976, 15, 2675-2681.

(k) Van Baar, J. F.; Vrieze, K.; Stufkens, D. J. J. Organomet. Chem. 1974, 81, 247-259.

(l) Bailey, N. A.; Jenkins, J. M.; Mason, R.; Shaw, B. L. J. Chem. Soc. Chem. Commun. 1965, 237-238.

(m) La Placa, S. J.; Ibers, J. A. Inorg. Chem. 1965, 4, 778-783.

(n) Cotton, F. A.;La Cour, T.; Stanilowski, A. G. J. Am. Chem. Soc. 1974, 96, 754-759.

References

(o) Cotton, F. A.; Day, V. W. J. Chem. Soc. Chem. Commun. 1974, 415-416.

(p) Cotton, F. A.; Stanislowski, A. G. J. Am. Chem. Soc. 1974, 96, 5074-5082.

(q) Harlow, R. L.; McKinney, R. J.; Ittel, S. D. J. Am. Chem. Soc. 1979, 101, 7496-7504.

(r) Brown, R. K.; Williams, J. M.; Schultz, A. J.; Stucky, G. D.; Ittel, S. D.; Harlow, R. L. J. Am. Chem. Soc. 1980, 102, 981-986.

(s) Brookhart, M.; Lamanna, W.; Humphrey, M. B. J. Am. Chem. Soc. 1982, 104, 2117-2126.

(t) Schultz, A. J.; Teller, R. G.; Beno, M. A.; Williams, J. M.; Brookhart, M.; Lamanna, W.; Humphrey, M. B. Science 1983, 220, 197-199.

(u) Dawoodi, Z.; Green, M.L.H.; Mtetwa, V.S.B.; Prout, K. J. Chem. Soc. Chem. Commun. 1982, 802-1982, 1410-1411.

(v) Schultz, A.; Williams, J. M.; Schrock, R. R.; Rupprecht, G.; Fellmann, J.D. J. Am. Chem. Soc. 1979, 101, 1593-1594.

(w) Calvert, R. B.; Shapley, J. R. J. Am. Chem. Soc. 1978, 100, 7726-7727.

(x) Dawkins, G. M.; Green, M.; Orpen, A. G.; Stone, F.G.A. J. Chem. Soc. Chem. Commun. 1982, 41-43.

(y) Beno, M. A.; Williams, J. M.; Tachikawa, M.; Muetterties, E.L. J. Am. Chem. Soc. 1981, 103, 1485-1492.

6. (a) For a general review of surface chemistry see: Somorjai, G. A., "Chemistry in Two Dimensions: Surfaces:, Cornell Univ. Press, Ithaca 1981. For a review of H_2 on transition metal surfaces see: Burch, R. Chem. Phys. Solids: Their Surfaces 1980, 8, 1-7.

(b) Maire, G.; Anderson, J.R.; Johnson, B. B. Proc. Roy. Soc. London, 1970, A320, 227-250.

(c) Schouten, F. C.; Kaleveld, E. W.; Bootsma, G. A. Surf. Sci. 1977, 63, 460-474.

References

(d) Firment, L. E.; Somorjai, G. A. J. Chem. Phys. 1977, 66, 2901-2913.

(e) Salmeron, M.; Somorjai, G. A. J. Chem. Phys. 1981, 85, 3635-3840.

(f) Madey, T. E.; Yates, J. R. Surf. Sci. 1978, 76, 397-414.

(g) Wittrig, T. S.; Szuromi, P. D.; Weinberg, W. H. J. Chem. Phys. 1982, 1, 116-123; ibid. 1982, 76, 3305-3315.

(h) Tsai, M. C.; Friend, C. M.; Muetterties, E. L. J. Am. Chem. Soc. 1982, 104, 2539-2543.

(i) Karpinsky, Z. J. Catal. 1982, 77, 118-137.

(j) Yates, J. T., Jr.; Zinck, J. J.; Sheard, S.; Weinberg, W. H. J. Chem. Phys. 1979, 70, 2266-2272.

(k) Hoffmann, F. M.; Felter, T. E.; Weinberg, W. H. J. Chem. Phys. 1982, 76, 3799-3808.

(l) Felter, T. E.; Hoffmann, F. M.; Thiel, P. A.; Weinberg, W. H. Surf. Sci. 1983, 80,

(m) Hoffmann, F. M.; Felter, T. E.; Thiel, P. A.; Weinberg, W. H. Surf. Sci. 1983, 80

(n) Weinberg, W. H. Surv. Progr. Chem. 1983, 10, 1-59.

(o) Somorjai, G. A. in "Robert A. Welch Foundation Conference on Chemical Research. XXV. Heterogeneous Catalysis", 1981, 83-138.

(p) Demuth, J. E.; Ibach, H.; Lehwald, S. Phys. Rev. Lett. 1978, 40, 1044-1047.

7. (a) Baetzold, R. J. Am. Chem. Soc. 1983, 105, 4271-4276; Shustorovich, E. J. Phys. Chem. 1983, 87, 14-17; Shustorovich, E.; Baetzold, R.; Muetterties, E. L. J. Phys. Chem. 1983, 87, 1100-1113.

Shustorovich, E. J. Am. Chem. Soc. 1980, 102, 5989-5993; J. Phys. Chem. 1982, 86, 3114-3120; Sol. State Commun. 1982, 44, 567-572.

See also Rev. 3b.

8. For an illuminating discussion of this problem see: Crabtree, R. H.; Hlatky, G. G. Inorg. Chem. 1980, 19, 571-572.

9. (a) Hoffmann, R. J. Chem. Phys. 1963, 39, 1397-1412.

(b) Hoffmann, R.; Lipscomb, W. N. J. Chem. Phys. 1962, 36, 2176-2195.

References

10. (a) Sevin, A. Nouv. J. de Chim. 1981, 5, 233-241; Sevin, A.; Chaquin, P. Nouv. J. Chem. 1983, 7,353-360.

(b) Dedieu, A.; Strich, A. Inorg. Chem. 1979, 18, 2940-2943.

(c) Kitaura, K.; Obara, S.; Morokuma, K. J. Am. Chem. Soc. 1981, 103, 2892-2892. Obara, S.; Kitaura, K.; Morokuma, K. to be published.

(d) Shestakov, A. F. Koordin. Khim. 1980, 6, 117-123.

(e) Gritsenko, O. V.; Bagaturyants, A. A.; Moiseev, I. I.; Kazanskii, V. B.; Kalechits, I. V. Kinetika i Katal. 1980, 21, 632-638. Kuzminskii, M. B.; Bagaturyants, A. A.; Zhidomirov, G. M.; Kazanskii, V. B. Kinetika i Katal. 1981, 22, 354-358. Gritsenko, O. V.; Bagaturyants, A. A.; Moiseev, I. I.; Kalechits, I. V. Kinetika i Katal. 1981, 22, 1431-1437. Bagaturyants, A. A.; Anikin, N. A.; Zhidomirov, G. M.; Kazanskii, V. B. Zh. Fiz. Khim. 1981, 55, 2035-2039. Zh. Fiz. Khim. 1982, 56, 3017-3022. Anikin, N. A.; Bagaturyants, A. A.; Zhidomirov, G. M.; Kazanskii, V. B. Zh. Fiz. Khim. 1982, 56, 3003-3007. Lebedev, V. L.; Bagaturyants, A. A.; Zhidomirov, G. M.; Kazanskii, V. B. Zh. Fiz. Khim. 1983, 57, 1057-1067. Bagaturyants, A. A. Zh. Fiz. Khim. 1983, 57, 1100-1106.

(f) Noell, J.O.; Hay, P. J. J. Am. Chem. Soc. 1982, 104, 4578-4584; Hay, P. J. J. Am. Chem. Soc. 1983, 105,

(g) Blomberg, M. R. A.; Siegbahn, P. E. M. J. Chem. Phys. 1983, 78, 986- Brandemark, U. B.; Blomberg, M. R. A.; Petterson, L. G. M.; Siegbahn, P. E. M. J. Phys. Chem. 1983,

11. Graham, M. A.; Perutz, R. N.; Poliakoff, M.; Turner, J. J. J. Organomet. Chem. 1982, 34, C34 (1972). Welch, J. A.; Peters, K. A.; Vaida, V. J. Phys. Chem. 1982, 86, 1941-1947.

12. Elian, M.; Hoffmann, R. J. Am. Chem. Soc. 1975, 14, 1058-1076.

13. See Ref. 12 for the orbitals of ML_4.

14. We assume a low-spin-singlet configuration for both ML_4 and CpM'L. For the orbitals of CpML and a discussion of its geometry and spin states see: Hofmann, P.; Padmanabhan, M. Organomet. 1983, ; see also Veillard, A.; Dedieu, A. Theor. Chim Acta.

References

15. Komiya, S.; Albright, T. A.; Hoffmann, R.; Kochi, J. K. J. Am. Chem. Soc. 1976, 98, 7255-7265. Tatsumi, K.; Hoffmann, R.; Yamamoto, A.; Stille, J.K. Bull. Chem. Soc. Japan, 1981, 54, 1857-1867. Hoffmann, R. IUPAC, "Frontiers of Chemistry", Pergamon Press, Oxford 1982, 247-263. Pearson, R. G. Acc. Chem. Res. 1971, 4, 152-160. "Symmetry Rules for Chemical Reactions", Wiley-Interscience, New York 1976, pp.286-405. Braterman, P. S.; Cross, R. J. Chem. Esc. Rov. 1973, 1, 271-294. Åkermark, B.; Johansen, H.; Roos, B.; Wahlgren, U. J. Am. Chem. Soc. 1979, 101, 5876-5883. Albright, T. A. Tetrahedron 1982, 38, 1339-1388. Balacz, A. C.; Johnson, K.H.; Whitesides, G. M. Inorg. Chem. 1982, 21, 2162-2174.

16. Elian, M.; Chen, M. M. L.; Mingos, D.M.P.; Hoffmann, R. J. Amer. Chem. Soc. 1976, 15, 1148-1155.

17. Ashcroft, N. W.; Mermin, N. D. "Solid State Physics", Saunders, Philadelphia, 1976. Kittel, C. "Introduction to Solid State Physics", J. Wiley and Sons, Inc., New York 1976. Wannier, G. H. "Elements of Solid State Theory" Cambridge University Press 1966.

18. A typical contemporary calculation on bulk Ni, using a method much better than ours, may be found in Wang, C. S.; Callasay, J. Phys. Rev. B 1977, 15, 298-306. There are some noticeable differences between our band structure and this one, in that in our calculation the DOS in the d band is more uniformly distributed, less peaked.

19. For an important early extended Hückel calculation of bulk Ni and the (111) surface see: Fassaert, D.J. M.; van der Avoird, A. Surf. Sci. 1976, 55, 291-312.

20. For calculations on the distribution of electrons in the bulk and on the surface see Dejonquères, M. C.; Cyrot-Lackmann, F. J. Chem. Phys. 1976, 64, 3707-3715; and Kahn, O.; Salem, L.

21. Hughbanks, T.; Hoffmann, R. J. Am. Chem. Soc. 1983, 105, 1150-1162. Wijeyesekera, S.; Hoffmann, R., to be published.

References

22. For other calculations on the Ni (111) surface see:

(a) Dempsey, D. G.; Grise, W. R.; Kleinman, L. Phys. Rev. B 1978, 18, 1550-1553. These computations obtain less of a charge shift between surface and inner layers that we do. Among the numerous calculations of surfaces we refer the reader to the following:

(b) Arlinghaus, F. J.; Gay, J. G.; Smith, J. R. Phys. Rev. B 1980, 21, 2055-2059. Gay, J. G.; Smith, J. R.; Arlinghaus, F. J. Phys. Rev. Lett. 1979, 42, 332-335. Smith, J. R.; Gay, J. G.; Arlinghaus, F. J.; Phys. Rev. B. 1980, 21, 2201-2221.

(c) Bisi, O.; Calandra, C. Surf. Sci. 1979, 83, 83-92.

(d) Feibelman, P. J.; Appelbaum, J. A.; Hamann, D. R. Phys. Rev. B 1979, 20, 1433-1443. Appelbaum, J. A.; Hamann, D. R. Sol. State Commun. 1978, 27, 881-883.

(e) Fulde, P.; Luther, A.; Watson, R. F. Phys. Rev. B 1973, 8, 440-452.

(f) Dempsey, D. G.; Kleinman, L. Phys. Rev. B 1977, 16, 5356-5366.

(g) Louie, S. G. Phys. Rev. Lett. 1978, 40, 1525-1528.

Experimental studies on the relative electron density of surface and inner atoms include:

(h) Citrin, P. H.; Wertheim, G. K.; Bayer, Y. Phys. Rev. Lett. 1978, 41, 1425-1428.

(i) Tran Minh Duc; Guillot, C.; Lassailly, Y.; Lecante, J.; Jugnet, Y.; Vedrine, J. C. Phys. Rev. Lett. 1979, 43, 789-792.

(j) Van der Veen, J. F.; Himpsel, F. J.; Eastman, D. E. Phys. Rev. Lett. 1980, 44, 189-198.

References

23. See also

(a) Feibelman, P. J.; Hamann, D. R. Solid State Commun. 1979, 31, 413-416.

(b) Desjonqueres, M. C.; Spanjaard, D.; Lassailly, Y.; Guillot, C. Solid State Commun. 1980, 34, 807-810.

24. $H_2 \cdots H_2$ interactions are dropped here, but they are anyway small at the intermolecular H···H contact of 2.49Å. When we eventually do CH_4 on the same surface, we will not drop $CH_4 \cdots CH_4$ interactions.

25. (a) Salem, L.; Leforestier, C. Surf. Sci. 1979, 82, 390-412.

(b) Nørskov, J. K.; Houmøller, A.; Johansson, P. K.; Lundqvist, B. I. Phys. Rev. Lett. 1981, 46, 257-260. Lundqvist, B. I.; Hellsing, B.; Homström, S.; Nordlander, P.; Perrson, M.; Nørskov, J. K. Int. J. Quant. Chem. 1983, XXIII, 1083-1090. Lundqvist, B. I.; Gunnarson, O.; Hjelmberg, H.; Nørskov, J. K. Surf. Sci. 1979, 89, 196-225. Lundqvist, B. I. "Vibrations at Surfaces", Ed. by Caudano, R.; Gilles, J. M.; Lucas, A. A., Plenum Publ. Co. 1982, pp.541-572. Lundqvist, B. I., to be published.

(c) Kobayashi, H.; Yoshida, S.; Kato, H.; Fukui, K.; Tamara, K. Surf. Sci. 1979, 79, 190-205.

(d) Andzelm, J. Surf. Sci. 1981, 108, 561-588. Andzelm, J.; Radzio-Andzelm, E. Chem. Phys. 1981, 61, 317-323.

(e) Charlot, M. F.; Kahn, O. Surf. Sci. 1979, 81, 90-108.

(f) Bohl, M.; Müller, H. Surf. Sci. 1983, 128, 117-127.

(g) Baetzold, R. Surf. Sci. 1975, 51, 1-13.

(h) Fritsche, H. G.; Mertins, G. Z. Phys. Chem. 1976, 257, 913-928.

(i) Anderson, A. B. J. Am. Chem. Soc. 1977, 99, 696-707.

References

(j) Van Santen, R. A. Rec. Trav. Chim. 1982, 101, 121-136.

(k) Salem, L.; Elliott, R. J. Mol. Struc. Theochem. 1982, 93, 75-84.

(l) Deuss, H.; van der Avoid, A. Phys. Rev. B. 1983, 8, 2441- ; see also Ref.18b.

(m) These two references contain calculations on CH_3, CH_2, CH on surfaces: Gavin, R. M.; Reutt, J.; Muetterties, E. A.; Proc. Natl. Acad. Sci. USA, 1981, 78, 3981-3985. Minot, C.; Van Hove, M. A.; Somorjai, G. A. Surf. Sci. 1982, 127, 441-460.

26. This way of thinking is related to the "surface amplitude patterns" developed by Minot, C.; Kahn, O.; Salem, L. Surf. Sci. 1980, 94, 515-527.

27. Actually the C—H bonds pointing toward the metal were taken as 1.10Å, so as to simplify the analysis. The other C—H bonds were 1.09 Å.

28. This trend has also been noted and explained by Baetzold in Ref. 21.

29. Ballhausen, C. J.; Gray, H. B. "Molecular Orbital Theory", W. A. Benjamin, Inc., New York 1965, p.125

30. McGlynn, S. P.; Van Quickenborne, L. G.; Kinoshita, M.; Caroll, D. G. "Introduction to Applied Quantum Chemistry", Holt, Rinehart and Winston, Inc., New York 1972.

31. Donohue, J. "The Structure of the Elements", R. E. Krieger, Malabar 1982.

32. Pack, J. D.; Monkhorst, H. J. Phys. Rev. B 1977, 16, 1748-1749.

SECURITY CLASSIFICATION OF THIS PAGE (When Data Entered)

REPORT DOCUMENTATION PAGE		READ INSTRUCTIONS BEFORE COMPLETING FORM
1. REPORT NUMBER: 1	2. GOVT ACCESSION NO.	3. RECIPIENT'S CATALOG NUMBER
4. TITLE (and Subtitle): C-H and H-H Activation in Transition Metal Complexes and on Surfaces		5. TYPE OF REPORT & PERIOD COVERED: Technical Report
		6. PERFORMING ORG. REPORT NUMBER
7. AUTHOR(s): J.-Y. Saillard and R. Hoffmann		8. CONTRACT OR GRANT NUMBER(s): N00014-82-K-0576
9. PERFORMING ORGANIZATION NAME AND ADDRESS: Department of Chemistry, Cornell University, Ithaca, New York 14853		10. PROGRAM ELEMENT, PROJECT, TASK AREA & WORK UNIT NUMBERS
11. CONTROLLING OFFICE NAME AND ADDRESS: Office of Naval Research, 800 Quincy Street, Arlington, Virginia		12. REPORT DATE
		13. NUMBER OF PAGES
14. MONITORING AGENCY NAME & ADDRESS (if different from Controlling Office)		15. SECURITY CLASS. (of this report)
		15a. DECLASSIFICATION DOWNGRADING SCHEDULE

16. DISTRIBUTION STATEMENT (of this Report)

This document has been approved for public release and sale; its distributions unlimited.

17. DISTRIBUTION STATEMENT (of the abstract entered in Block 20, if different from Report)

18. SUPPLEMENTARY NOTES

Accepted for publication in the Journal of the American Chemical Society

19. KEY WORDS (Continue on reverse side if necessary and identify by block number)

C-H Activation, H-H Activation, catalysis

20. ABSTRACT (Continue on reverse side if necessary and identify by block number)

The breaking of the H-H bond in H_2 and a C-H bond in CH_4 on both discrete transition metal complexes and on Ni and Ti surfaces is studied, and the essential continuity and similarity of the physical and chemical processes in two cases is demonstrated. We begin with an orbital analysis of oxidative addition, delineating four basic interactions: H-H or C-H $\sigma \rightarrow$ M electron transfer, the reverse M $\rightarrow \sigma^*$ transfer (both weakening the σ bond, forming the M-H bond), a repulsive interaction between σ and metal filled orbitals, and a re-

DD FORM 1 JAN 73 1473 EDITION OF 1 NOV 65 IS OBSOLETE

S/N 0102-LF-014-6601

SECURITY CLASSIFICATION OF THIS PAGE (When Data Entered)

20. arrangement of electron density at the metal. The molecular cases analyzed in detail are $d^6 ML_5$, $d^8 ML_4$ and $CpM'L$. Coordinative unsaturation is necessary, and consequently $\sigma \rightarrow M$ electron transfer dominates the early stages of the reaction. Steric effects are important for CH_4 reaction. Activation in angular ML_4 or $CpM'L$ is achieved through a destabilized yz MO, and $d^{10} ML_3$, ML_2 candidates for activation are described. For our study of the surface we develop tools such as projections of the density of states and crystal orbital overlap populations - the extended structure analogues of a population analysis. These allow a clear understanding of what happens when an H_2 or a CH_4 molecule approaches a surface. Because of the higher energy of the occupied metal orbitals on the surface the $M \rightarrow \sigma^*$ interaction leads the reaction. There are great similarities and some differences between the activation acts in a discrete complex and on a surface.